CHARLES UNIVERSITY

FACULTY OF PHARMACY IN HRADEC KRÁLOVÉ

DPT. OF PHARMACEUTICAL CHEMISTRY AND PHARMACEUTICAL ANALYSIS

DESIGN, SYNTHESIS AND EVALUATION OF HETEROCYCLIC COMPOUNDS WITH POTENTIAL ANTIMICROBIAL ACTIVITY IV

Diploma Thesis

Amirhossein Fekri

Supervisor: doc. PharmDr. Jan Zitko, Ph.D.

Consultant: Mgr. Vinod Sukanth Kumar Pallabothula

Hradec Králové, 2023

ACKNOWLEDGEMENT

I would like to thank my supervisor, doc. PharmDr. Jan Zitko, Ph.D. my consultant
Mgr. Vinod S. K. Pallabothula (doctoral student) and our head of department,
prof. PharmDr. Martin Doležal, Ph.D. for their guidance and support, and finally my
family for their endless love and trust in my abilities.

Hradec Králové, 2023   Amirhossein Fekri

Hradec Králové, 2023   Amirhossein Fekri

Contents

List of Abbreviations

aa	Amino acid
ACN	Acetonitrile
Ala	Alanine
Arg	Arginine
aaRS	Aminoacyl-tRNA synthetase
AspRS	Aspartyl-tRNA synthetase
ATP	Adenosine triphosphate
β-Ala	Beta-alanine
BCG	Bacillus Calmette-Guérin
CoA	Coenzyme A
ClpC1-ClpP	Caseinolytic protease complex
DCM	Dichloromethane
DMSO	Dimethyl sulfoxide
eq	Equivalent (molar)
EtOAc	Ethyl acetate
EtOH	Ethanol
Glu	Glutamate
EPRS	Glutamyl-prolyl-tRNA synthetase
H-bond	Hydrogen bond
HBA	Hydrogen bond acceptor
HBD	Hydrogen bond donor
Hex	Hexane
HPLC	High-performance liquid chromatography
hsProRS	*Homo sapiens* prolyl-tRNA synthetase
IleRS	Isoleucyl-tRNA synthetase
IR	Infrared spectroscopy
L-Cys	*L*-cysteine
LeuRS	Leucyl-tRNA synthetase
M.	Mycobacterium
Me	Methyl
MeO	Methoxy
MetRS	Methionine-tRNA synthetase
MIC	Minimum inhibitory concentration
min	Minute
MOE	Molecular operating environment
m.p.	Melting point
MshC	Mycothiol ligase
Mtb	*Mycobacterium tuberculosis*

mtLeuRS	Mycobacterial leucyl-tRNA tRNA synthetase
mtProRS	Mycobacterial prolyl-tRNA synthetase
N.D..	Not determined
NMR	Nuclear magnetic resonance
P.	*Plasmodium*
PanD	Aspartate decarboxylase
PDB	Protein Data Bank
Phe	Phenyl alanine
PLIF	Protein-Ligand Interaction Fingerprints
pncA	Pyrazinamidase gene
POA	Pyrazinoic acid
PP_i	Pyrophosphate
Pro	Proline
Pro-AMP	Prolyl-adenylate complex
ProRS	Prolyl-tRNA synthetase
PZA	Pyrazinamide
PZAase	Pyrazinamidase
rpsA	Gene encoding Ribosomal protein S1
TB	Tuberculosis
THF	Tetrahydrofurane
Thr	Threonine
TLC	Thin layer chromatography
TMS	Tetramethylsilane
tRNA	Transfer RNA
tRNA^{Leu}	Leucyl-tRNA
tRNA^{Pro}	Prolyl-tRNA

ABSTRACT: (English)

Charles University, Faculty of Pharmacy in Hradec Králové

Department of Pharmaceutical Chemistry and Pharmaceutical Analysis

Thesis title: Design, synthesis and evaluation of heterocyclic compounds with potential antimicrobial activity IV

Candidate: Amirhossein Fekri

Supervisor: doc. PharmDr. Jan Zitko, Ph.D.

Consultant: Mgr. Vinod S. K. Pallabothula

Tuberculosis has remained one of the deadliest infectious diseases worldwide caused by a single infectious agent, the rapid growth of resistance to anti-tubercular drugs hinders the successful control and treatment of TB worldwide, which challenges the scientific community to develop new drugs to improve currently available treatment. This diploma thesis represents the design, synthesis, and biological evaluation of two series of compounds including cyclized (pyrazine-oxazinone) and carboxamide derivatives as potentially active antimycobacterial agents sharing a pyrazine core as common structural features that could potentially target mycobacterial aspartate decarboxylase (PanD) and prolyl-tRNA synthetase (mtProRS), respectively. Synthesis of final compounds was achieved through individual reaction steps involving acylation of methyl 3-aminopyrazine-2-carboxylate for preparation of a common intermediate which in turn was used for the synthesis of final compounds. All the final compounds were analyzed by ^{1}H and ^{13}C-NMR spectroscopy, IR spectroscopy, and determination of melting point. Out of 14 final compounds, eventually, seven were tested for in-vitro activity against five mycobacterial strains. Overall, five out of seven compounds tested have shown mild to moderate antimycobacterial activity against some mycobacterial strains. Moreover, in-silico molecular docking of a small library of virtually prepared ligands was performed to identify new potential candidates for targeting mtProRS. The overall outcome of this experimental study encourages/supports further investigation of newly identified potential candidates for the development of new antimycobacterial drugs with improved selectivity toward mycobacterium and lower toxicity to humans.

ABSTRAKT: (Czech)

Univerzita Karlova, Farmaceutická fakulta v Hradci Králové

Katedra farmaceutické chemie a farmaceutické analýzy

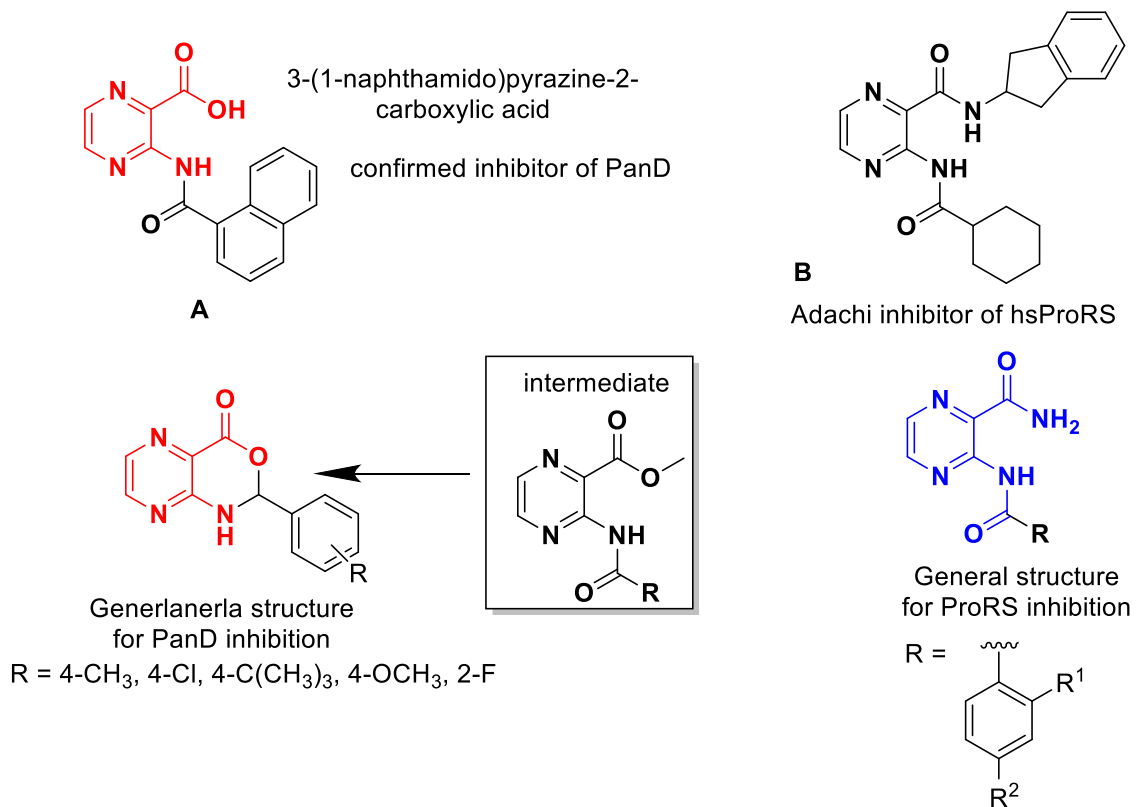|	
Název:	Návrh, syntéza a hodnocení heterocyklických sloučenin s potenciální antimikrobní aktivitou IV
Kandidát:	Amirhossein Fekri
Školitel:	doc. PharmDr. Jan Zitko, Ph.D.
Konzultant:	Mgr. Vinod S. K. Pallabothula

Tuberkulóza zůstává celosvětově jednou z nejsmrtelnějších infekčních nemocí způsobených jediným infekčním agens, rychlý růst rezistence na antituberkulotika brání úspěšné kontrole a léčbě TBC po celém světě, což je výzvou pro vědeckou komunitu, aby vyvinula nová léčiva ke zlepšení v současnosti dostupné léčby. Tato diplomová práce představuje návrh, syntézu a biologické hodnocení dvou sérií sloučenin včetně cyklizovaných (pyrazin-oxazinon) a karboxamidových derivátů jako potenciálně aktivních antimykobakteriálních látek sdílejících společný strukturní fragment pyrazinového jádra, které by mohly potenciálně cílit na mykobakteriální aspartát dekarboxylázu (PanD) a prolyl-tRNA syntetázu (mtProRS). Syntézy finálních sloučenin bylo dosaženo prostřednictvím jednotlivých reakčních kroků zahrnujících acylaci methyl-3-aminopyrazin-2-karboxylátu pro přípravu běžného meziproduktu, který byl následně použit pro syntézu finálních sloučenin. Všechny konečné sloučeniny byly analyzovány ^{1}H a ^{13}C-NMR spektroskopií, IR spektroskopií a stanovením teploty tání. Ze 14 finálních sloučenin bylo nakonec sedm testováno na aktivitu *in vitro* proti pěti mykobakteriálním kmenům. Celkově pět ze sedmi testovaných sloučenin vykázalo mírnou až střední antimykobakteriální aktivitu proti některým mykobakteriálním kmenům. Kromě toho bylo provedeno *in silico* molekulové dokování malé knihovny virtuálně připravených ligandů za účelem identifikace nových potenciálních kandidátů pro cílení na mtProRS. Celkový výsledek této experimentální studie povzbuzuje/podporuje další zkoumání nově identifikovaných potenciálních kandidátů na vývoj nových antimykobakteriálních léčiv se zlepšenou selektivitou vůči mykobakteriím a nižší toxicitou pro člověka.

AIM OF WORK

In this work, we aim to design, synthesize, and test two series of compounds including cyclized (pyrazine-oxazinone) and pyrazine-carboxamide derivatives as potentially active antimycobacterial agents (refer to Figure 1). Final structures contained the pyrazine core, the aromatic nucleus of the structurally simple, first-line anti-tubercular, pyrazinamide. The unclear mechanism of action of pyrazinamide and its many proposed molecular targets inspired us to further develop analogues with specific structural modifications toward two interesting targets, PanD (aspartate decarboxylase) and ProRS (prolyl-tRNA synthetase). We prepare common intermediates for both end targets. The general structure for PanD inhibition activity was inspired by the work of Ragunathan *et al* where they attached a bulky naphthamido group at the 3rd position of pyrazine core, refer to the structure **A** in Figure 1.[1] On the other hand, the general structure for prolyl-tRNA synthetase inhibition activity was based on Adachi ligand, 3-(cyclohexanecarboxamido)-*N*-(2,3-dihydro-1H-inden-2-yl)pyrazine-2-carboxamide, which is the confirmed inhibitor of the human homolog of the enzyme (refer to structure B in Figure 1).[2] Moreover we manually prepare a database of ligands for docking into mtProRS. As the importance of second and fourth position substituents for targeting the mycobacteria was demonstrated by our research group, the prepared database of ligands are typically substituted with short alkyl or halogen at position 2' or/and 4' with few exceptions which are substituted at position 3' of the phenyl ring.[3, 4]

3-(1-naphthamido)pyrazine-2-carboxylic acid

confirmed inhibitor of PanD

A

B

Adachi inhibitor of hsProRS

intermediate

Generlanerla structure
for PanD inhibition
R = 4-CH$_3$, 4-Cl, 4-C(CH$_3$)$_3$, 4-OCH$_3$, 2-F

General structure
for ProRS inhibition

R =

Figure 1. General structure for PanD inhibition indicated by red colour on the left. General structure for ProRS inhibition indicated by blue colour on the right.

1. INTRODUCTION

1.1. Tuberculosis

Tuberculosis (TB) is a contagious disease transmitted when an infected person releases infectious droplets into the air by coughing or sneezing.[5, 6] TB is caused by the rod-shaped *Mycobacterium tuberculosis* (*Mtb*). Individuals who are exposed to *Mtb* may develop either primary active disease or latent infection, which is clinically asymptomatic and may progress to active disease when the immune system gets compromised.[7] TB commonly affects the lungs, however, it can also affect other organs, such as pleura, lymph nodes, bones, joints, or urogenital tract which in that case is referred to as extrapulmonary TB. The latter form of TB accounts for 15% of all TB cases and is more challenging to diagnose and treat.[8-10] Classical symptoms of TB includes fever, productive cough, and weight loss, among others.[7] The pathophysiology of TB is complex, involving several immune system responses. The most important TB infection hallmarks are summarized in Figure 2 below.[11]
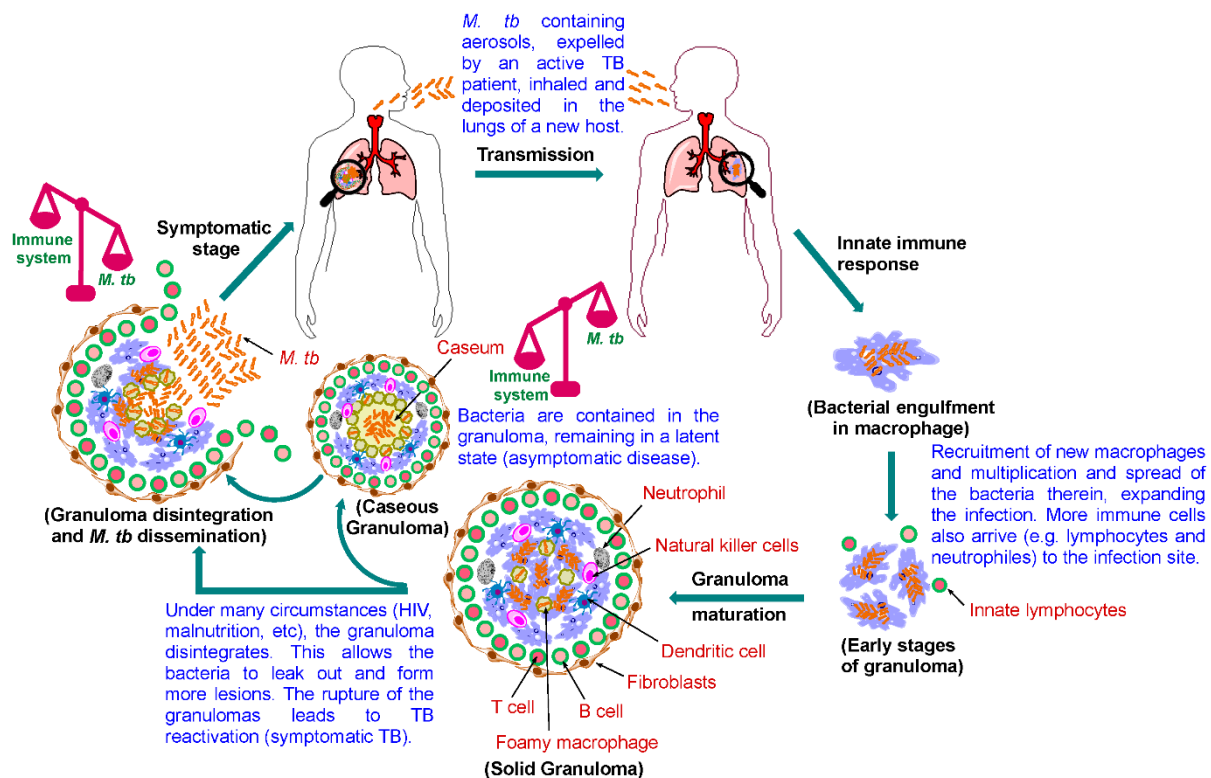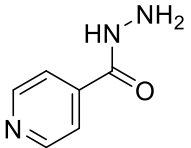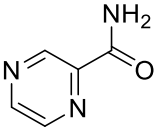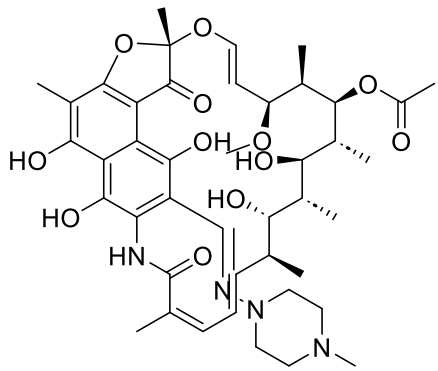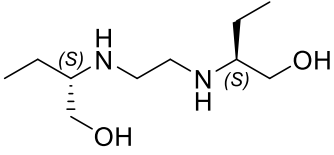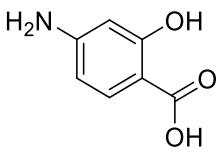

Figure 2. Pathophysiology of pulmonary TB. Taken from a publication [11]
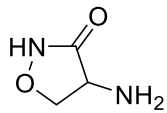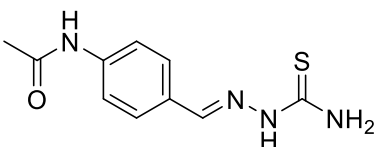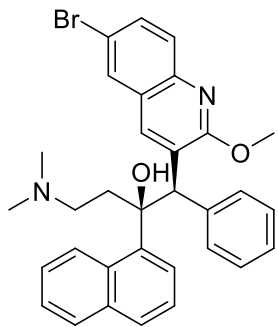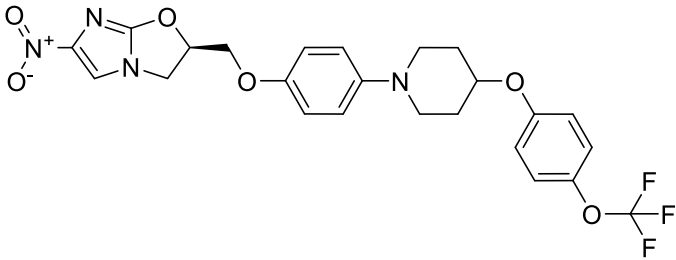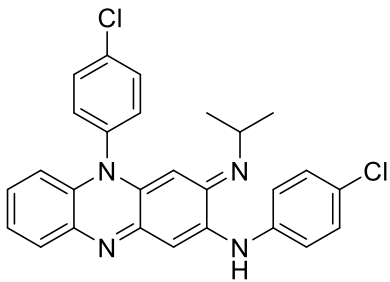
Available anti-tubercular agents are divided into first- and second-line. Agents and their mechanism of action are summarized in Table 1. Treatment-susceptible TB is treated by giving the four first-line agents together for a period of two months, which is known as the induction

phase, and then treatment is continued for another four months with isoniazid and rifampicin, which is known as the continuation phase, the second line agents are res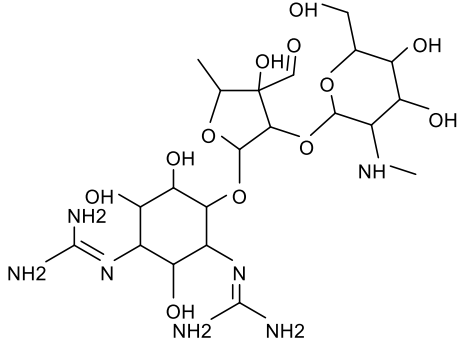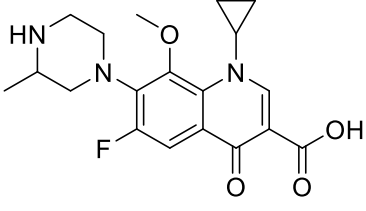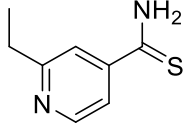erved for treatment-resistant TB cases. Other less effective drugs are also classified as second-line agents. The lengthy, complex treatment of TB results in poor adherence to treatment as a consequence, the emergence of antimicrobial resistance.[6, 12, 13]

Table 1. First- and second-line anti-tubercular drugs, their chemical structures, and mechanism of action.[6, 12, 14, 15]

First-line antituberculars		
Name	**Chemical structure**	**Mechanism of action**
Isoniazid		Inhibits InhA (enoyl acyl carrier protein reductase)
Pyrazinamide		Number of suggested molecular targets are described
Rifampicin		Inhibits DNA-dependent RNA polymerase

Ethambutol		Inhibits arabinosyl-transferases
Second-line antituberculars		
Aminoglycosides (Streptomycin, Kanamycin, Amikacin)	 Streptomycin	Bind to the 30s ribosomal subunit, inhibit translation and protein synthesis (protein synthesis inhibitor)
Fluoroquinolones (Levofloxacin, Gatifloxacin Moxifloxacin)	 Gatifloxacin	Inhibit topoisomerases II & IV (nucleic acid synthesis inhibitor)
Ethionamide		Inhibits enoyl-ACP reductase enzyme
4-Aminosalicylic acid		Inhibits Dihydrofolate reductase (after metabolic activation)

D-Cycloserine		Inhibits cell wall synthesis
Thioacetazone		Inhibits mycolic acid synthesis
Bedaquiline		Inhibits ATP synthase
Delamanid		Inhibits synthesis of mycolic acid
Clofazimine		Exact target not yet known

Our design rationale is based on the first-line anti-tubercular agent pyrazinamide (PZA). Structurally, PZA is a nicotinamide analogue. It has been used in therapy since 1952. It plays a vital role in TB treatment regimen as it shortens the course of drug-sensitive TB treatment from 9 to 6 months due to the unique sterilizing activity against semi-dormant, non-replicating mycobacteria.[16, 17] Despite its long-term availability in the market, PZA still attracts research interest due to its ambiguous mode of action. Several theories have been proposed regarding

how PZA exerts its antimycobacterial activity. Interestingly, the antimycobacterial activity of pyrazinamide was first evaluated in infected animals, and it was found that pyrazinamide possesses a potent activity in vivo. [18] On the contrary, no activity was observed after testing in a standard mycobacterial culture medium of Mtb at near neutral pH. Further studies demonstrated that the culture medium is needed to be mildly acidic (pH of 5.8) for PZA to inhibit the growth of Mtb.[16] It is confirmed that pyrazinamide acts as a pro-drug that is converted to its biologically active form, pyrazinoic acid, by the enzyme pyrazinamidase/nicotinamidase coded by the pncA gene. Mutations in pncA gene are most commonly associated with resistance to pyrazinamide. It was believed that pyrazinamide is active only at acidic pH based on the old theories suggesting that pyrazinamide shows improved activity in acidic media thus TB lung lesions are acidic, the first proposed mechanism of action for pyrazinamide was based on an ionophore model. This model describes PZA as a prodrug that enters Mtb by passive diffusion across the cellular envelope to the cytoplasm (pH 7.2), where it is converted to its biologically active metabolite POA (pKa of 2.9) by the catalytic activity of enzyme PZase.[16, 19] Following exposure to an acidic environment such as activated phagosome or acidified culture medium, POA becomes protonated and subsequently shuttles protons from the extracellular acidic environment into the bacilli which consequently result in collapse of membrane energetics and cytoplasmic acidification due to accumulation of protons.[19] However, this mode of action has been challenged by recent findings about inhibitory effect of PZA and POA on the growth of Mtb at neutral pH, suggesting that acidic pH is not strictly associated with antimycobaacterial activity of the drug.[16] Moreover, TB lesions are not necessarily of acidic character, however, they are present with various range of pH from acidic to alkaline. Subsequent studies demonstrated that, even under near-neutral culture conditions the improved PZA activity could be achieved in the presence of other factors including *pncA* overexpression (that is, overexpression of the activating enzyme), inhibition of efflux pumps to prevent POA export from the bacilli, exposure of bacilli to conditions such as alkaline pH, low temperature, nutrient limitation, and hypoxia.[18, 20] Worth mentioning that, POA does not cause rapid collapse of membrane potential or cytoplasmic acidification in Mtb unlike bona fide ionophores, such as carbonyl cyanide m-chlorophenyl hydrazine.[21] It was proved that in order for POA to achieve its MIC, it must be available at much higher concentrations in the cytoplasm. According to experimental data, POA failed to alter the membrane potential of Mtb in the medium at pH 5.8 over the period that was evaluated even at concentrations 10-fold above the MIC.[16]

According to the fact that PZA/POA is also active at neutral pH and that TB lung lesions are not necessarily acidic, it was hypothesized that the failure to isolate POA-resistant mutants was due to the acidic pH used in the selection media. Therefore, there was an attempt to recover PZA/POA-resistant mycobacteria on neutral pH agar. Moreover, results from whole genome sequencing revealed missense mutations in the gene the aspartate decarboxylase PanD, which is involved in the biosynthesis of the essential cofactor Coenzyme A. PanD catalyses the decarboxylation of L-aspartate to β-alanine, which is the rate-limiting step in this pathway.[21-23] Recent findings suggest the vulnerability of this pathway both *in vitro* and *in vivo* therefore it could be considered a promising approach to target this cofactor synthesis pathway via inhibition of PanD activity by novel therapeutic agents.[21]

Pyrazinamide interferes with the function of different targets that are involved in various cellular processes in mycobacteria, such as energy production, trans-translation (via interference with small ribosomal protein S1 ((RpsA) and metabolic pathways [pantothenate/coenzyme A (PanD)] which are essential for survival of the pathogen.[16, 18]

## 1.2. Aspartate decarboxylase (PanD)

Amino acid biosynthesis is essential for the survival and pathogenesis of Mtb. Therefore, one of the approaches applied in antibacterial drug discovery is targeting metabolic processes that are ideally specific for the pathogen. Aspartate decarboxylase is an enzyme responsible for catalyzing the conversion of L-aspartate to β-alanine, which subsequently is utilized as a precursor for the synthesis of pantothenate (commonly known as vitamin B5). Pantothenate is an essential cofactor involved in many critical metabolic processes, such as fatty acid synthesis and ATP production. In addition, pantothenate is required for the synthesis of coenzyme A (CoA), which is involved in the metabolism of fats, carbohydrates, and proteins, essential for energy production. The latter biosynthetic pathway represents an interesting target for antibacterial drug discovery as pantothenate is not synthesized *de novo* by humans.[24, 25] POA interferes with CoA biosynthesis by blocking PanD-mediated conversion of aspartate to β-Ala.[26] Interestingly, POA has a dual on-target mechanism. In addition to acting as a very weak inhibitor of PanD's enzymatic activity, binding of POA to PanD promotes the degradation of the protein by the caseinolytic protease complex ClpC1-ClpP.[24, 27] ClpC1 is an unfoldase that recognizes proteins containing various C-terminal tags and delivers these proteins for degradation to the ClpP protease. The ClpC1-ClpP complex is responsible for proteome housekeeping and regulation of the protein level of certain proteins.[28] Taken together,

mechanism of action studies suggest that POA may act as a bacterial target 'degrader', and thus PZA to be the first antibacterial to act as a selective target degrader.[29, 30]

However, it must be noted that Mtb strains lacking *panD* gene are still susceptible to PZA, suggesting that aspartate decarboxylase is not the only molecular target for PZA.[31] This is elucidated by recent studies on PZA/POA-resistant mycobacteria which are recovered on neutral pH agar. Whole-genome sequencing demonstrated missense mutations in PanD. Interestingly, the frequency of panD polymorphisms in clinical isolates is low, although the reason for this is still not clear. Missense mutations in the Coenzyme A biosynthetic pathway gene PanD encoding Aspartate Decarboxylase cause PZA resistance in *vitro* and *in vivo* showing that cenzyme A biosynthesis is essential in Mtb both *in vitro* and *in vivo*.[32] Therefore, resistance caused by missense mutations in PanD would then be due to a lack of drug binding. Indeed, outcomes of biophysical analyses demonstrated that POA could bind to recombinant wild-type PanD but not proteins containing POA-resistance mutations. Last but not least, panD poly-morphisms associated with PZA resistance are rare in clinical isolates of Mtb.[21]

1.2.1. Derivatives of 3-amino-POA as inhibitors of PanD

Recent available studies reporting the design and synthesis of 3-amino-POA analogues as inhibitors of Mtb PanD, refer to Figure 3. Enzymatic activity was assessed by β-Ala production evaluation. Their best inhibitor was 3-(1-naphthamido)pyrazine-2-carboxylic acid (bearing the bulky naphtamido moiety). The latter inhibitor had 1000-fold increase in enzymatic inhibition compared to POA, and moderate improvement in anti-mycobacterial activity, approximately 4-folds when compared to POA against M. bovis BCG, which is an attenuated variant of Mtb. Such analogues inhibit PanD via one on-target mechanism, which is enzymatic inhibition.[1]
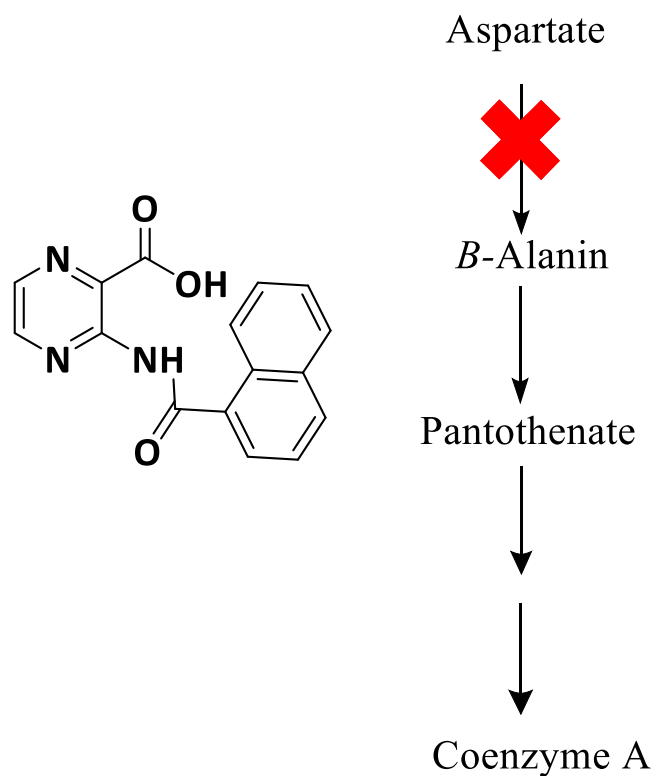
Figure 3. The chemical structure of 3-(1-naphthamido)pyrazine-2-carboxylic acid, the best inhibitor of Mtb PanD reported by Ragunathan et al and its mechanism of action.[1]

As mentioned earlier in the Aim of the work section, we designed our final products containing cyclized derivatives of pyrazine pharmacophore. These cyclized derivatives contain a fused lactone ring to the pyrazine that could potentially act as prodrugs which are depicted below in Figure 4. We hypothesized that our newly synthesized compounds which may get cleaved metabolically to produce the pyrazinoic acid derivatives may exhibit a similar structure skeleton to the reference molecules that in return can potentially inhibit mycobacterial PanD[1].

$R = 4\text{-}CH_3, 4\text{-}Cl, 4\text{-}C(CH_3)_3, 4\text{-}OCH_3, 2\text{-}F$
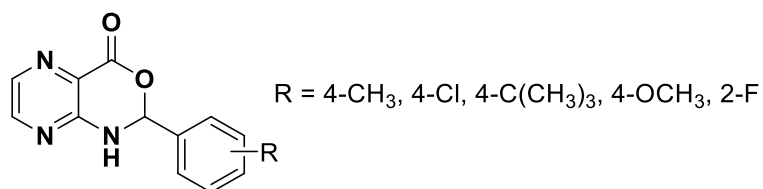
Figure 4. Demonstration of R substituted pyrazine-oxazinone derivatives.

1.3. Aminoacyl-tRNA synthetases

Protein synthesis has always been an important target for antimicrobial drugs. The aim of drug discovery is to design agents that affect different stages in the process of protein synthesis. Aminoacyl-tRNA synthetases (aaRSs) are a class of enzymes belonging to the adenylate-forming enzyme group responsible for maintaining the fidelity of protein synthesis by pairing the amino acids to their related tRNA in an ATP-dependent manner. In other words, they charge tRNA with the related aa. The charged tRNA is subsequently utilized at ribosome during the process of translation.[33-35] the role of aaRSs is not limited only to translation; they get involved in different processes such as proofreading of mature tRNA, transcriptional regulations, mitochondrial RNA cleavage, cytokine-like activities, and biosynthesis of alarmones (bacterial second messengers vital for surviving stress conditions). aaRSs could be targeted for the treatment of multiple human diseases as they are involved in various physiological and pathological processes including post-translational modifications, autoimmune diseases, angiogenesis, fibrosis, and neuromuscular disorders.[4, 36] Moreover they could be targeted in various inflammatory diseases including lung cancer, breast cancer, and ovarian cancer that are associated with overexpression and higher catalytic activity of a particular aaRSs.[37] Apart from human-related disease, the aaRSs have been known as perspective targets for the treatment of various infectious diseases including protozoal, fungal, parasites, and bacterial infections. The divergence between prokaryotic and eukaryotic cytoplasmic aaRS offers the possibility to design selective inhibitors.[33, 38] Therefore recently various types of aaRSs inhibitors have been found such as substrate mimetics, Trojan horses, induced-fit inhibitors, and reaction hijacking inhibitors.[34, 39, 40] Sequence similarities and conserved binding motifs allow the design of multi-target inhibitors, especially for aaRSs within the same subclass. As an example, we can mention L-Cys:mycothiol ligase (MshC), which is inhibited by inhibitors of MetRS. Except for oxaboroles targeting the editing site of MtLeuRS, the reported inhibitors of mycobacterial aaRSs bind to the catalytic site (ATP- binding site, aminoacyl-binding site, or both. The aim is to design compounds by a combination of an ATP (or adenine) mimicking fragment with improved pharmacokinetic properties and an aminoacyl mimicking fragment with affinity to one or more aaRSs and at the same time making use of the (often subtle) interspecies differences between aaRSs to achieve selectivity.[35] Recently various compounds have been extensively investigated for targeting various aaRSs. Obafluorine is a natural product, that has been reported as a novel covalent inhibitor of bacterial threonyl-tRNA synthetase (ThrRS).[41]

Obafluorine

Tavaborole

**2-(quinolin-2-ylsulfanyl)-acetamide scaffold**
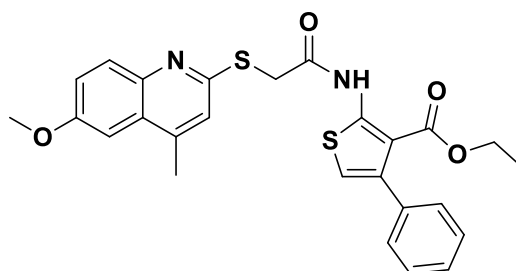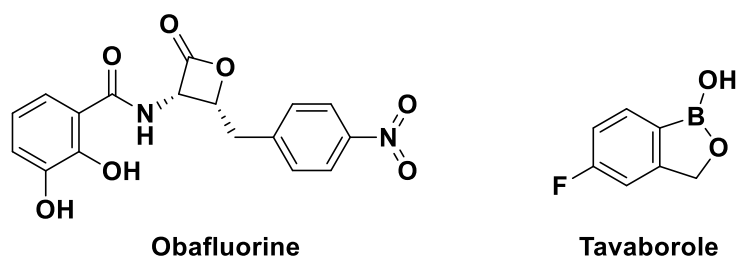
Among more recent advancements in antimicrobial research, it is worth to mention 2-(quinolin-2-ylsulfanyl)-acetamide scaffold which has been discovered as a potential dual-target inhibitor of aaRSs for the treatment of tuberculosis.[42] Among boron-based compounds (benzaoxaboreles e.g. tavaborole) targeting leucyl-tRNA synthetase (LeuRS), including an antibiotic that recently has successfully passed phase II clinical trials as a potential therapeutic agent for the treatment of tuberculosis. Interestingly it was found that benzoxaboroles do not bind directly to their target LeuRS, instead they are prodrugs that enable their activation by forming a reversible LeuRS inhibition adduct with AMP, ATP, or the terminal adenosine of the tRNA[Leu].[43] Currently, there are three inhibitors of various aaRS in therapy including mupirocin as a competitive inhibitor of bacterial isoleucyl-tRNA synthetase (IleRS) which has been used for the treatment of skin infection,[44] tavaborole (AN2690) is a benzoxaborole derivative act as an irreversible inhibitor of fungal leucyl-tRNA synthetase (LeuRS) approved for the treatment of onychomycosis, and halofuginone as a non-competitive inhibitor of protozoal prolyl-tRNA synthetase (ProRS) in p.falciparum.[35, 45] Moreover halofuginone is indicated for the treatment of scleroderma as an orphan drug approved by FDA.[46]

1.4. Prolyl-tRNA Synthetase

In the antimycobacterial research, the potential of aaRSs inhibitors has been rather undervalued. The most studied aaRSs in mycobacteria spc. is LeuRS with at least four structural types of inhibitors, followed by AspRS and TyrRS. Lately, Prolyl-tRNA synthetase (ProRS) has been extensively investigated by our search group as potential target for the development of novel

antimycobacterial drugs.[3, 4] Prolyl-tRNA synthetase (ProRS) is responsible for catalyzing the synthesis of prolyl-tRNA^{Pro} utilizing ATP, L-proline, and tRNA^{Pro} as a substrate which could be done by a two-step reaction. The initial step involved the formation of enzyme-bound prolyl-adenylate complex (Pro-AMP) and pyrophosphate (PP$_i$) in the presence of ATP. The later step of the reaction is done by transferring the activated amino acid to the 3′-end of tRNA^{Pro}, forming aminoacylated tRNA (Pro-tRNA^{Pro}).[34, 39, 40] Halofuginone as a confirmed ProRS inhibitor occupies both the proline (Pro) and the 3′-end of related tRNA binding sites in an ATP-dependent manner. Halofuginone has shown to have anti-fibrosis and anti-tumor activities in addition to its brilliant antimalarial activity.[2, 47, 48] According to recently available investigations, many hsProRS inhibitors are identified based on pyrazinamide pharmacophore among which there is an ATP-competitive inhibitor that works in a proline-dependent fashion.[2] Moreover a novel series of pyrazinamide ProRS inhibitors have been discovered by our research group. The outcome of this study was finding of a novel drug-like ProRS inhibitor with a unique binding mode to hsProRS in proline-dependent manner. This latter inhibitor was effective in a cellular context, Thus, the series of ProRS inhibitors are considered to be a forward step for development with differentiation from earlier mentioned halofuginone.[4]

It is worth mentioning that recent studies demonstrated upregulation of EPRS in hepatocellular carcinoma which is associated with enhanced proliferation of cancer cells. Glutamyl-prolyl-tRNA synthetase (EPRS) is a dual-function enzyme responsible for catalysing the formation of charged glutamyl-tRNA and prolyl-tRNA in the cytoplasm. The human ProRS (hsProRS) activity is located at the C-terminal region of this protein and inhibition of this enzyme has been recognized as a promising approach for the treatment of hsProRS -related diseases. Therefore recently, a novel ATP-competitive ProRS inhibitor has been synthesized as a potential therapeutic agent for the treatment of multiple myeloma.

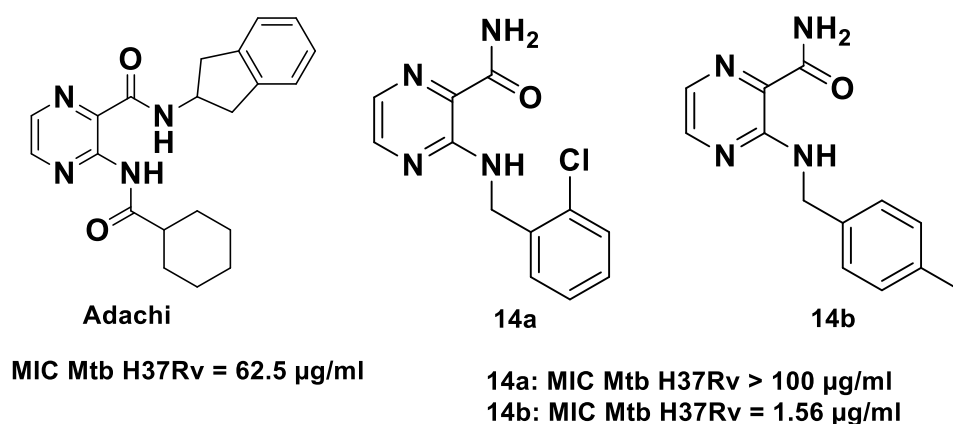
Bersiporicin   NCP26
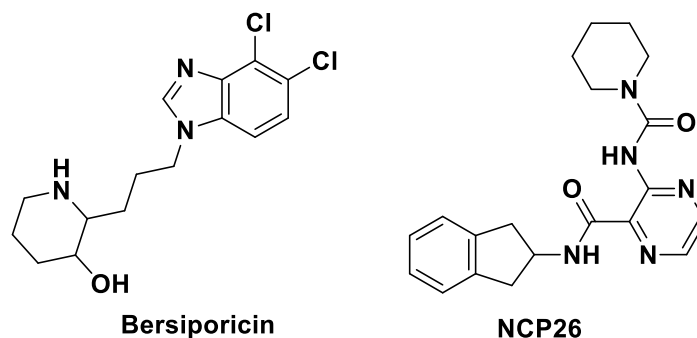
This latter inhibitor known as NCP26 contains pyrazinamide scaffold as the main structural feature and interestingly possess high structural similarity to Adachi ligand which is the

confirmed inhibitor of hsProRS.[49, 50] Moreover, among recent advancements in treatment of fibrosis, is worth mentioning the development of a novel prolyl-tRNA synthetase inhibitor, Bersiporicin (DWN12088) which is under clinical evaluation for the treatment of idiopathic pulmonary fibrosis.[51]

1.4.1. Derivatives of 3-amino-PZA as inhibitors of ProRS

Derivatives of 3-aminopyrazine-2-carboxamide with simple substituents were prepared previously by our research group, refer to Figure 5. The design was based on Adachi ligand, which is the confirmed ATP-competitive inhibitor of human prolyl-tRNA synthetase (hsProRS). Adachi ligand binds to the ATP site of the enzyme in the presence of *L*-proline, mimicking the interactions of the adenine core. The binding affinity of the synthesized derivatives toward hsProRS was evaluated by Thermal shift assay and crystallographic studies. It was concluded that 2'-substitution of such structures favors halogen atoms particularly chlorine (Cl) or/and short alkyl substituents such as methyl. [2]

Adachi

MIC Mtb H37Rv = 62.5 µg/ml

14a

14b

14a: MIC Mtb H37Rv > 100 µg/ml
14b: MIC Mtb H37Rv = 1.56 µg/ml

Figure 5. Derivatives of 3-amino-PZA (**14a**, **14b** compound numbers from the article)[52] and reference compound of Adachi, and their antimycobacterial activity.

Available experimental data by our research group demonstrated that newly synthesized derivatives with 2'-substitution on benzene ring could also bind to hsProRS. which is very well confirmed according to the results from thermal shift assay and picture from crystallographic studies. The overlay of simplified derivatives of 3-aminopyrazine-2-carboxamide with Adachi ligand in the active site of the enzyme is very well depicted in Figure 6, although the affinity is weaker in comparison to Adachi ligand.[2] The weaker affinity could have been due to the missing carbonyl oxygen (in the 3'-substituent), which is found to be essential for higher

binding affinity toward the enzyme via the formation of strong hydrogen bond interaction between the carbonyl oxygen and hydrogen of Thr of the enzyme as depicted in Figure 6.[2, 3]
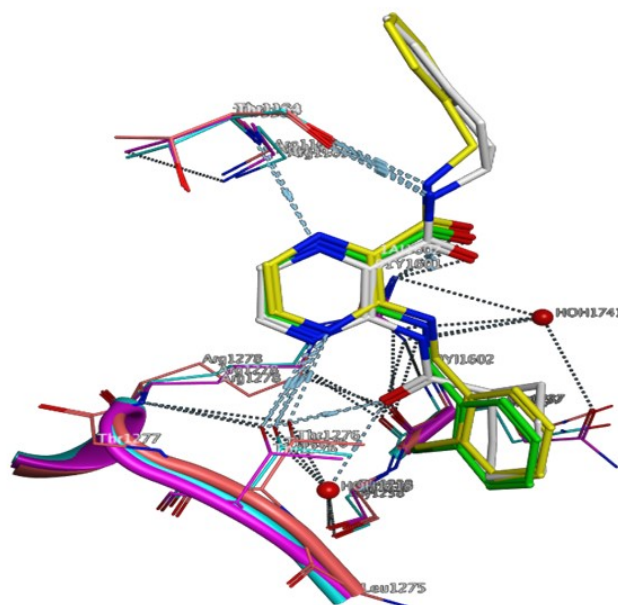
Figure 6. Overlay of Adachi hsProRS inhibitor (white carbons) with in-house 2'-sbustituted derivatives of 3-aminopyrazine-2-carboxamide, in hsProRS.[4]
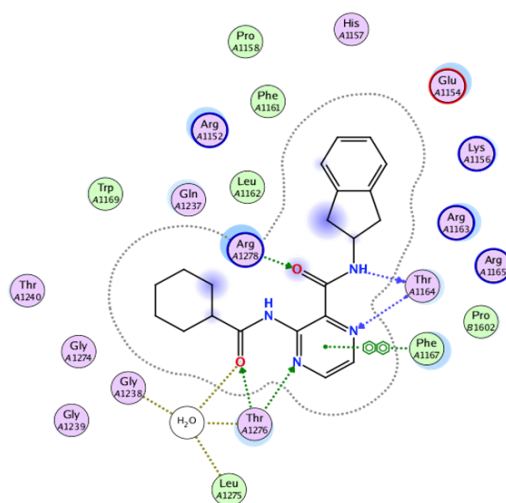
Figure 7. 2D ligand-protein interaction diagram demonstrating the confirmed hsProRS inhibitor and importance of carbonyl oxygen interaction with threonyl (Thr1276) for binding to hsProRS.

As a result of experimental studies, it was found that derivatives with 2'-substitution on phenyl ring with short alkyl or halogen possess no anti-mycobacterial activity, however, the 4'-substituted derivatives possess moderate *in vitro* activity against mycobacteria but no binding affinity to hsProRS. This could justify the distinction between the structure of human and mycobacterial protein. Therefore 4'-substituted derivatives could potentially bind to mtProRS.

For this reason, the structure is further optimized by the synthesis of repurposed compounds with carbonyl oxygen similarly as reference hsProRS inhibitor (Adachi) to improve the binding affinity towards ProRS by preserving the carbonyl group in the structure and also substitution at position 4' with short alkyl particularly methyl or halogen to maintain potential antimycobacterial activity. Despite that target studies are still not available, but one of the best previously studied compounds showing promising activity against mycobacteria is compound 15 (numbering in the original publication) from the article which is depicted below in Figure 8. This latter compound shows interaction with the homology model of mtProRS and will be subjected to further studies and evaluation.[2, 3]

MIC Mtb H37Ra: 3.91 µg/mL
Cytotoxicity HepG2: 100* µM
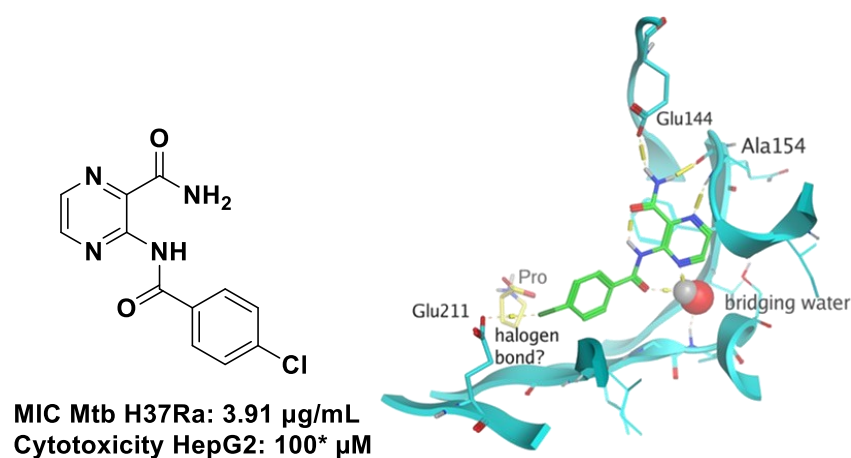
Figure 8. Compound **15** docked (induced fit docking) into the homology model of mtProRS. A – Ligand-receptor interactions in 3D.[3]

Based on recently available results from experimental studies, my diploma thesis was focused on the synthesis of another group of compounds from the same series with a hybrid structure of 2 previously described derivatives of 3-aminopyrazine-2-carboxamide where the carbonyl group is preserved and benzene ring is substituted at position 2' and 4', concomitantly to improve the binding affinity and antimycobacterial activity (refer to Figure 9). The aim is to synthesize new target compounds with a higher selectivity toward mycobacterial ProRS and *in vitro* antimycobacterial activity but lack significant toxicity on human cells (mediated by interaction with hsProRS).
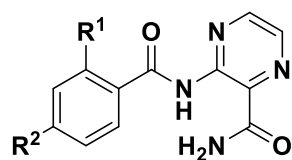
R¹, **R²**=short alkyl and/or halogen

Figure 9. Newly synthesized derivatives with potentially improved binding affinity while maintaining antimycobacterial activity.

2. EXPERIMENTAL SECTION

2.1. Instrumentation and General Information

All reagents and solvents (unless stated otherwise) were purchased from Merck (Taufkirchen, Germany) and used without further purification. Reaction progress and purity of products were monitored using Silica 60 F_{254} TLC plates (Merck, Darmstadt, Germany). Flash chromatography of the final compounds was performed on a puriFlash XS420+ (Interchim, Montluçon, France) with original columns (spherical silica, 30 μm) provided by the same company. The mobile phase was ethyl acetate (EtOAc) in hexane (Hex), gradient elution 0–100%, and detection was performed by UV-VIS detector at 254 nm and 280 nm. The NMR spectra were recorded either on a Varian VNMR S500 (Varian, Palo Alto, CA, USA) at 500 MHz for ^{1}H and 126 MHz for ^{13}C or on a Jeol JNM-ECZ600R at 600 MHz for ^{1}H and 151 MHz for ^{13}C. The spectra were recorded in DMSO-d_6 or CDCl$_3$ at ambient temperature. The chemical shifts reported as δ values in ppm are indirectly referenced to tetramethylsilane (TMS) via the solvent signal (2.49 for ^{1}H and 39.7 for ^{13}C in DMSO-d_6; 7.26 for ^{1}H and 77.2 for ^{13}C in CDCl$_3$). IR spectra were recorded on a NICOLET 6700 FT-IR spectrophotometer (Nicolet, Madison, WI, USA) using the ATR-Ge method. Elemental analysis was done on a Vario MICRO cube Element Analyzer (Elementar Analysensysteme, Hanau, Germany) with values given as a percentage. The purity of the newly synthesized compounds with Fluorine atoms was measured using a Shimadzu LC20 chromatograph (Shimadzu, Kyoto, Japan) coupled with a PDA detector (SPD-M20A) on the ZORBAX ECLIPSE XDB - C18 (3.0 × 50 mm, 1.8 μm, Agilent Technologies, U.S.A) column using an acetonitrile/water mobile phase mixture in gradient mode. Data were processed using LabSolutions software (v. 5.92, Shimadzu, Kyoto, Japan). The stock solution of each compound (1.0 mg/mL) was prepared by dissolving the appropriate amount in methanol. Working solutions were prepared by diluting the stock solutions with the acetonitrile/water mixture (1:1, *v/v*) to a concentration of 50 μg/mL. The PDA detector acquired spectra from 190 to 380 nm, and a wavelength of 260 nm was employed for purity evaluation. Yields are given in percentage and refer to the amount of pure product after all purification steps. Melting points were determined in open capillary on a Stuart SMP30 melting point apparatus (Bibby Scientific Limited, Staffordshire, UK) and are uncorrected.

LogP values were calculated using ChemDraw v20.0. (PerkinElmer Informatics, Waltham, MA, USA). *In silico* calculations were performed in Molecular Operating Environment (MOE) 2022.02 (Chemical Computing Group Inc., Montreal, QC, Canada) under Amber10:EHT forcefield.

2.2. Chemistry

2.2.1. Synthesis of Substituted 3-benzamidopyrazine-2-carboxylates (Intermediate esters)
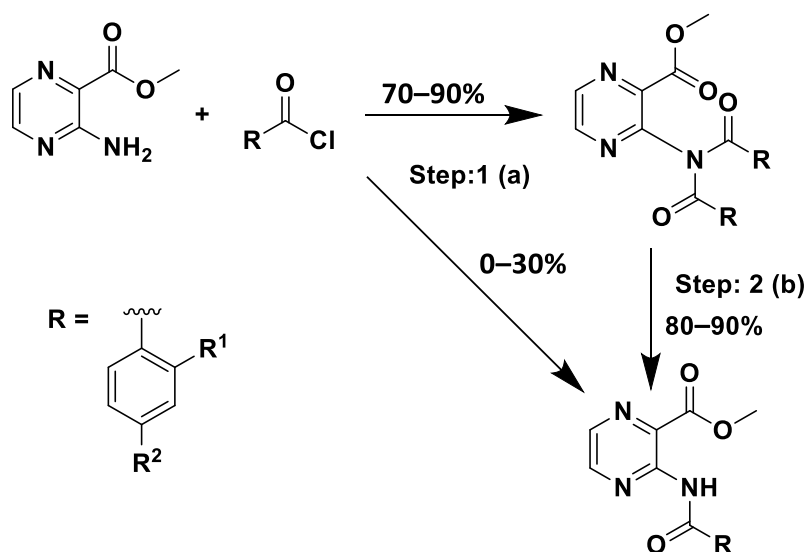
**Scheme 1.** Synthetic procedures for preparation of common intermediate.
(a) ACN solvent; Pyridine as Base; 70 °C; 24 h
(b) Hydrazine hydrate; THF solvent; Isopropanol as catalyst; Reflux for 1 h

Step 1: Acylation of Methyl 3-Aminopyrazine-2-Carboxylate

4 mmol (613 mg) of starting material (methyl 3-aminopyrazine-2-carboxylate; was weighed in a round bottom flask and dispersed in 20 mL of acetonitrile (ACN). The reaction mixture was stirred at room temperature for 5 min, and then 2.5 eq (0.8 mL) of anhydrous pyridine was added as a base. The reaction mixture was stirred for another 5 min and 2.2 eq of corresponding acyl chloride was added dropwise. The reaction temperature was increased to 70 °C and refluxed for 24 h. Reaction progress was checked on TLC using 1:1 Hex;EtOAc as mobile phase. Once the reaction was complete with full consumption of the starting material, the solvent was evaporated under reduced pressure. The crude reaction mixture of diacylated (undesired product) and monoacylated (desired product) products was obtained. Both diacylated and monoacylated products were purified by automated flash chromatography using EtOAc in Hex as eluent. After purification, both the diacylated and monoacylated products were separated into two fractions in two different round bottom flasks for evaporation of the residual solvents of the mobile phase by rotary evaporator under reduced pressure. After evaporation, pure diacylated and monoacylated products were obtained. The typical yield of this reaction for the variously substituted diacylated product was 80–90% however the typical yield of this reaction for the synthesis of variously substituted monoacylated product was 0–30%.

Step 2: Reduction of diacylated side-product to mono-acylated product
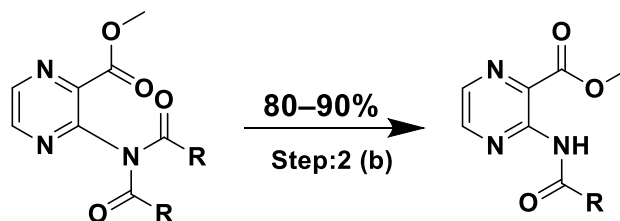
Scheme 2. Synthesis of 3-benzamidopyrazine-2-carboxylates by reduction of a diacylated side-product.
(b) Hydrazine hydrate; THF solvent; Isopropanol as catalyst; Reflux for 1 h

The conversion of diacylated (undesired product) to monoacylated (desired) product was carried out by a reduction reaction. Into a round bottom flask containing 10 mL of tetrahydrofuran (THF), 1 mmol of diacylated product was added and heated to reflux, then 3 mL of isopropanol was added as a catalyst which was followed by the addition of 1 mL (1eq) of 1M hydrazine hydrate in THF. The reaction mixture was refluxed for 1h. Once the reaction was complete, the solvent was evaporated, and the final product was dispersed in water. A few drops of sulphuric acid were added to the water for acidification and the product was extracted to EtOAc using a separatory funnel. The typical yield of this reduction reaction to monoacylated intermediate was 80–90%.

2.2.2. Synthesis of Pyrazine-oxazinone derivatives (Final compounds)

Cyclisation of Intermediate esters
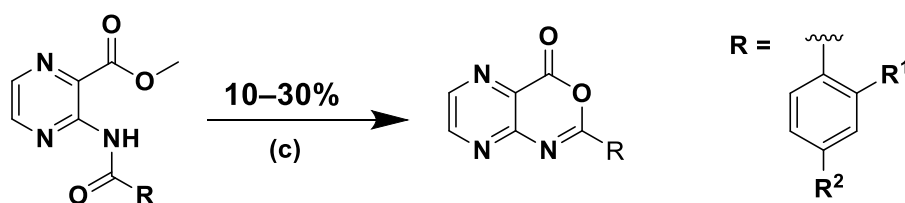
Scheme 3. Synthesis of cyclized derivatives from intermediate esters.
(c) Anhyd. toluene as solvent; triethylamine as base; 80 °C upto 6 h;
1,2-dibromotetrachloroethane; triphenylphosphine

1 mmol of the monoacylated intermediate (substituted methyl 3-benzamidopyrazine-2-carboxylate, 153 mg) was weighed and added into a 50 ml round bottom flask containing 15ml of anhydrous toluene as a solvent. The sample mixture with a magnetic stir bar was placed on a magnetic stirrer device at room temperature. 1.1 equivalent of triphenylphosphine (288 mg) was weighed and added to the reaction mixture followed by 3.0 equivalent (300 μL) of triethylamine was added and the reaction mixture was heated up to 80 °C under condenser with continuous stirring. After 10 min, 1.1 equivalent of 1,2-dibromotetrachloroethane (358 mg) was weighed and dissolved in a few mL of toluene in a separate flask and subsequently added dropwise to the reaction mixture. The reaction mixture was constantly stirred for 5 to 6 hours at 80 °C. Once the reaction was complete, the reaction mixture was filtered to remove the triethylammonium chloride residues. Afterwards, the solvent used during the reaction was evaporated from the reaction mixture by rotavapor under reduced pressure. The solid precipitate was obtained following evaporation which was subsequently washed off with ethanol (EtOH) and transferred to a beaker containing acetonitrile (ACN) as a solvent for recrystallization to remove trace impurities from the final product. The mixture was heated up to boiling temperature. Once the precipitate fully dissolved in ACN, the mixture was cooled down and filtration was followed. After filtration pure crystals were obtained of final yield was 10–30%.

2.2.3. Synthesis of 3-benzamidopyrazine-2-carboxamide derivatives (Final compounds)

Acylation of 3-Aminopyrazine-2-carboxamide
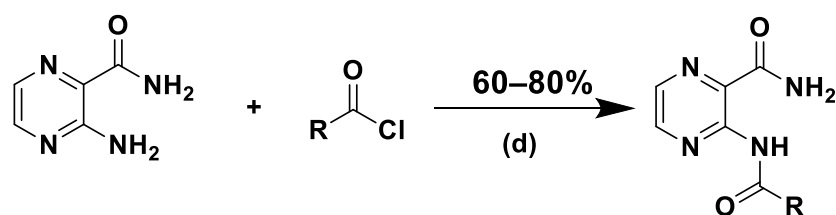
Scheme 4. Synthesis of 3-benzamidopyrazine-2-carboxamide derivatives.
(d) ACN solvent; Pyridine as Base; 50 °C; 24 h

In a dry round bottom flask, 3 mmol of starting material (3-aminopyrazine-2-carboxamide) was weighed. Afterwards, 10 ml of ACN was added as a solvent to dissolve the starting material. 1 ml of pyridine was added as a base to the reaction mixture. The reaction mixture was stirred constantly for 10 minutes at room temperature. After running the reaction for 10 min, 2.2 eq. of substituted benzoyl chloride was added to the reaction mixture. The reaction mixture was

heated up to 50 °C and maintained for 24h under constant stirring. Reaction progress was checked under TLC using 1:1 Hex; EtOAc. After full consumption of the starting material, the solvent present in the reaction mixture was evaporated under reduced pressure using a rotary evaporator. Following evaporation, a crude reaction mixture was obtained. The crude reaction mixture was purified by flash chromatography using 1:1 Hex; EtOAc as gradient mobile phase. The yield of this reaction was typically 60–80% across variously substituted derivatives.

2.3. Biological Assays
2.3.1. *In Vitro* biological evaluation on Mycobacterium species

Microdilution assay (Microplate Alamar Blue Assay (MABA)) was performed as described in our group's publication.[3] The initial antimycobacterial assay was performed with fast-growing *Mycolicibacterium* smegmatis DSM 43465 (ATCC 607), *Mycolicibacterium aurum* DSM 43999 (ATCC 23366); non-tuberculous (atypical) mycobacteria, namely *Mycobacterium avium* DSM 44,156 (ATCC 25291) and *Mycobacterium kansasii* DSM 44,162 (ATCC 12478), from German Collection of Microorganisms and Cell Cultures (Braunschweig, Germany) and with the virulent strain of *Mycobacterium tuberculosis* H37Ra ITM-M006710 (ATCC 9431) from Belgian Coordinated Collections of Microorganisms (Antwerp, Belgium) also according to the method published[53]. The technique used for activity determination was microdilution broth panel method using 96-well microtiter plates.

The cultivation medium was Middlebrook 7H9 broth (Merck, Steinheim, Germany) enriched with 0.4% of glycerol (Merck, Steinheim, Germany) and 10% of Middlebrook OADC growth supplement (Himedia, Mumbai, India). Mycobacterial strains were cultured on Middlebrook 7H9 agar and suspensions were prepared in Middlebrook 7H9 broth. Final density was adjusted to value 1.0 according to McFarland scale and diluted in a ratio 1:20 (for fast-growing mycobacteria) or 1:10 (for *M. tuberculosis*) with broth. Tested compounds were dissolved in DMSO (Merck, Steinheim, Germany) then Middlebrook broth was added to obtain a concentration of 2000 µg/mL. Standards used for activity determination were isoniazid (INH), rifampicin (RIF) and ciprofloxacin (CIP) (Merck, Steinheim, Germany). Final concentrations were reached by binary dilution and addition of mycobacterial suspension and were set as 500, 250, 125, 62.5, 31.25, 15.625, 7.81 and 3.91 µg/mL. Isoniazid was diluted in the range of 500–3.91 µg/mL for screening against fast-growing mycobacteria and in the range of 1–0.0078 µg/mL for screening against *M. tuberculosis*. Rifampicin final concentrations ranged from 50 to 0.39 µg/mL for fast-growing mycobacteria and from 1 to 0.0078 µg/mL for *M. tuberculosis*. Ciprofloxacin was used for screening antimycobacterial activity with the final concentrations

1–0.0078 μg/mL. The final concentration of DMSO did not exceed 2.5% (v/v) and did not affect the growth of *M. smegmatis*, *M. aurum* or *M. tuberculosis*. Positive (broth, DMSO, bacteria) and negative (broth, DMSO) growth controls were included. Plates were sealed with polyester adhesive film and incubated in dark at 37 °C without agitation. The 0.01% solution of resazurin sodium salt was added after 48 hours of incubation for *M. smegmatis*, after 72 hours of incubation for *M. aurum*, after 96 h of incubation for *M. avium* and *M. kansasii*, and after 120 hours of incubation for *M. tuberculosis*, respectively. After the addition of the dye, the microtitration plates were further incubated for 2.5 hours for *M. smegmatis*, 4 hours for *M. aurum*, 5–6 h for *M. avium* and *M. kansasii*, and 18 hours for *M. tuberculosis* before the activity was determined. The antimycobacterial activity was expressed as minimum inhibitory concentration (MIC) and the value was read based on stain color change (blue color – inhibition of growth; pink color – growth). All experiments were conducted in duplicate.

2.4. MONOGRAPHS OF FINAL COMPOUNDS

Compound 1

Chemical structure:
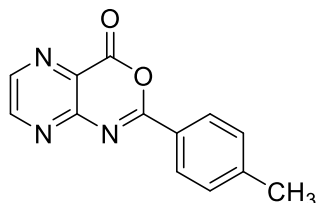
Laboratory Code: 4-Me LAC

Chemical Name: 2-(*p*-tolyl)-4*H*-pyrazino[2,3-*d*][1,3]oxazin-4-one

Chemical Formula: $C_{13}H_9N_3O_2$

Molecular weight: 239.23 g/mol

*Yield: 24%; 57 mg

Appearance: white, solid

m.p.: Not determined

^{1}H NMR: (600 MHz, CDCl$_3$) δ 8.97 (d, *J* = 2.1 Hz, 1H, PzH), 8.82 (d, *J* = 2.1 Hz, 1H, PzH), 8.49 – 8.17 (m, 2H, ArH), 7.45 – 7.31 (m, 2H, ArH), 2.47 (s, 3H, CH$_3$).

^{13}C NMR: (151 MHz, CDCl$_3$) δ 161.64, 157.49, 155.15, 151.57, 145.65, 145.49, 130.47, 129.99, 129.60, 126.14, 22.00.

Elemental analysis:

Theoretical: C, 65.27; H, 3.79; N, 17.56

Experimental: C, 65.20; H, 3.95; N, 17.64

IR (ATR-Ge, cm^{-1}): 2922, 1769(C=O, COO), 1609, 1573, 1557, 1536, 1018

Compound 2

Chemical structure:
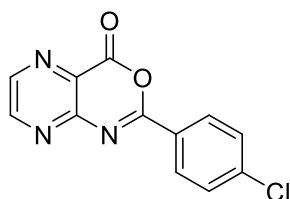
Laboratory Code: 4-Cl LAC

Chemical Name: 2-(4-chlorophenyl)-4*H*-pyrazino[2,3-*d*][1,3]oxazin-4-one

Chemical Formula: $C_{12}H_6ClN_3O_2$

Molecular weight: 259.65 g/mol

*Yield: 27%; 70 mg

Appearance: white, solid

m.p.: 277.1–279.6 °C

¹H NMR: (600 MHz, DMSO-d_6) δ 9.06 (d, J = 2.2 Hz, 1H, PzH), 8.90 (d, J = 2.2 Hz, 1H, PzH), 8.28–8.23 (m, 2H, ArH), 7.75–7.70 (m, 2H, ArH).

¹³C NMR: (151 MHz, DMSO-d_6) δ 158.72, 156.63, 153.64, 150.77, 145.14, 138.34, 130.96, 129.92, 129.00, 128.12

Elemental analysis:

Theoretical: C, 55.51; H, 2.33; Cl, 13.65; N, 16.18

Experimental: C, 55.56; H; 2.57; N; 15.98

IR (ATR-Ge, cm⁻¹): 3096, 1770(C=O, COO), 1611, 1504, 1539, 1489, 1028

Compound 3

Chemical structure:
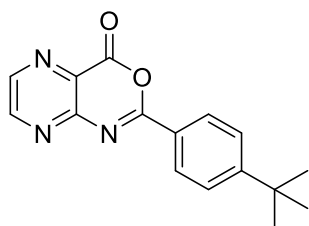
Laboratory Code: 4-tertBu LAC

Chemical Name: 2-(4-(*tert*-butyl)phenyl)-4*H*-pyrazino[2,3-*d*][1,3]oxazin-4-one

Chemical Formula: $C_{16}H_{15}N_3O_2$

Molecular weight: 281.32 g/mol

*Yield: 25%; 70 mg

Appearance: white, solid

m.p.: 215.5–218.2 °C

^{1}H NMR: (600 MHz, DMSO-d_6) δ 9.04 (d, *J* = 2.2 Hz, 1H, PzH), 8.87 (d, *J* = 2.2 Hz, 1H, PzH), 8.22–8.16 (m, 2H, ArH), 7.71–7.64 (m, 2H, ArH), 1.35 (s, 9H, *t*-BuH).

^{13}C NMR: (151 MHz, DMSO-d_6) δ 159.74, 157.53, 156.96, 154.17, 151.03, 145.08, 131.48, 128.47, 126.71, 126.10, 40.06, 34.99, 30.77.

Elemental analysis:

Theoretical: C, 68.31; H, 5.37; N, 14.94

Experimental: C, 68.11; H, 5.14; N, 15.09

IR (ATR-Ge, cm^{-1}): 2972, 2876, 1770 (C=O, COO), 1605, 1559, 1540, 1469, 1052

Compound 4

Chemical structure:
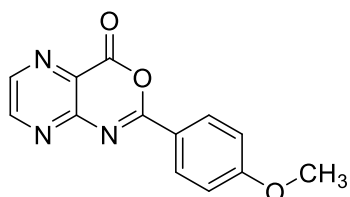
Laboratory Code: 4-MeO LAC

Chemical Name: 2-(4-methoxyphenyl)-4*H*-pyrazino[2,3-*d*][1,3]oxazin-4-one

Chemical Formula: $C_{13}H_9N_3O_3$

Molecular weight: 255.23 g/mol

*Yield: 23%; 59 mg

Appearance: Yellow, solid

m.p.: 206.1–208.5 °C

^{1}H NMR: (600 MHz, DMSO-d_6) δ 9.01 (d, J = 2.4 Hz, 1H, PzH), 8.83 (d, J = 2.3 Hz, 1H, PzH), 8.24–8.19 (m, 2H, ArH), 7.20–7.15 (m, 2H, ArH), 3.89 (s, 3H, OCH$_3$).

^{13}C NMR: (151 MHz, DMSO-d_6) δ 163.69, 159.63, 157.55, 154.34, 151.01, 144.72, 131.18, 130.72, 121.45, 114.71, 55.69.

Elemental analysis:

Theoretical: C, 61.18; H, 3.55; N, 16.46

Experimental: Not determined

IR (ATR-Ge, cm^{-1}): 2848 (CH$_3$), 1770 (C=O, CONH), 1600, 1530, 1513, 1015

Compound 5

Chemical structure:
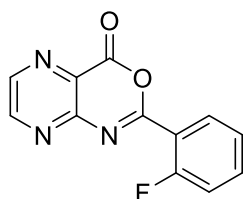
Laboratory Code: 2-F LAC

Chemical Name: 2-(2-fluorophenyl)-4*H*-pyrazino[2,3-*d*][1,3]oxazin-4-one

Chemical Formula: $C_{12}H_6FN_3O_2$

Molecular weight: 243.20 g/mol

*Yield: 28%; 68 mg

Appearance: White, solid

m.p.: 213.5–215.2 °C

^{1}H NMR: (600 MHz, DMSO-*d*₆) δ 9.07 (d, *J* = 2.2 Hz, 1H, PzH), 8.92 (d, *J* = 2.2 Hz, 1H, PzH), 8.20–8.12 (m, 1H, ArH), 7.80–7.74 (m, 1H, ArH), 7.51–7.43 (m, 2H, ArH).

^{13}C NMR: (151 MHz, DMSO-*d*₆) δ 160.80 (d, *J* = 259.4 Hz), 157.63 (d, *J* = 4.7 Hz), 157.33, 153.77, 151.08, 145.71, 135.58 (d, *J* = 9.1 Hz), 131.56, 125.06 (d, *J* = 3.6 Hz), 118.01 (d, *J* = 8.5 Hz), 117.50 (d, *J* = 21.7 Hz).

Elemental analysis:

Theoretical: C, 59.27; H, 2.49; F, 7.81; N, 17.28

IR (ATR-Ge, cm^{-1}): 3078, 1770(C=O), 1614, 1563, 1537, 1401, 1076

HPLC: 100% pure, 5 to 70% ACN/Water gradient

Compound 6

Chemical structure:
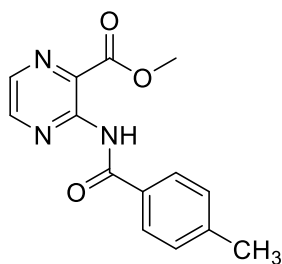
Laboratory Code: 4-Me E

Chemical Name: methyl 3-(4-methylbenzamido)pyrazine-2-carboxylate

Chemical Formula: $C_{14}H_{13}N_3O_3$

Molecular weight: 271.28 g/mol

*Yield: 80%; 217 mg

Appearance: Beige solid

m.p.: 158.9–161.2 °C

^{1}H NMR: (500 MHz, DMSO-d_6) δ 11.31 (s, 1H, NHCO), 8.71 (d, J = 2.4 Hz, 1H, PzH), 8.55 (d, J = 2.4 Hz, 1H, PzH), 7.96–7.90 (m, 2H, ArH), 7.38–7.32 (m, 2H, ArH), 3.75(s, 3H, OCH$_3$), 2.39 (s, 3H, CH$_3$)

^{13}C NMR: (126 MHz, DMSO-d_6) δ 166.00, 164.92, 146.02, 145.20, 142.82, 139.73, 138.44, 130.09, 129.12, 128.16, 52.35, 21.09

Elemental analysis:

Theoretical: C, 61.99; H, 4.83; N, 15.49

Experimental: C, 61.81; H, 4.78; N, 15.41

IR (ATR-Ge, cm^{-1}): 3313, 1687 (C=O, CONH), 1579, 1492, 1467, 1441, 1115.

Compound 7

Chemical structure:
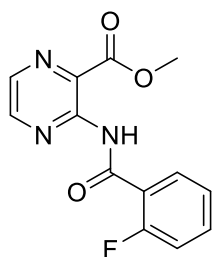
Laboratory Code: 2-F E

Chemical Name: Methyl 3-(2-fluorobenzamido)pyrazine-2-carboxylate

Chemical Formula: $C_{13}H_{10}FN_3O_3$

Molecular weight: 275.24 g/mol

*Yield: 85%; 234 mg

Appearance: Beige solid

m.p.: 123.2–125.4 °C

^{1}H NMR: (600 MHz, DMSO-d_6) δ 11.42 (s, 1H, NHCO), 8.70 (d, J = 2.5 Hz, 1H, PzH), 8.57 (d, J = 2.5 Hz, 1H, PzH), 7.69 (t, 1H, ArH), 7.66–7.60 (m, 1H, ArH), 7.39–7.33 (m, 2H, ArH), 3.80 (s, 3H, OCH$_3$)

^{13}C NMR: (151 MHz, DMSO-D_6) δ 165.40, 164.09, 159.89 (d, J = 251.2 Hz), 145.95 (d, J = 17.3 Hz), 145.83, 140.73 (dd, J = 24.9, 7.0 Hz), 138.39, 134.23, 130.71 (d, J = 10.2 Hz), 125.18 (d, J = 17.0 Hz), 123.35 (d, J = 13.1 Hz), 116.89 (d, J = 19.0 Hz), 53.01.

Elemental analysis:

Theoretical: C, 56.73; H, 3.66; F, 6.90; N, 15.27

IR (ATR-Ge, cm^{-1}): 3254, 1712 (C=O, CONH), 1610, 1506, 1453, 1127.

Compound 8

Chemical structure:
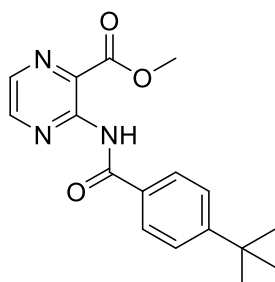
Laboratory Code: 4t-butyl E

Chemical name: methyl 3-(4-(*tert*-butyl)benzamido)pyrazine-2-carboxylate

Chemical Formula: $C_{17}H_{19}N_3O_3$

Molecular weight: 313.36 g/mol

*Yield: 83%; 260 mg

Appearance: Beige solid

m.p.: 114.3-116.6 °C

¹H NMR: (600 MHz, DMSO-d_6) δ 11.31 (s, 1H, NHCO), 8.71 (d, J = 2.4 Hz, 1H, PzH), 8.55 (d, J = 2.4 Hz, 1H, PzH), 7.99–7.94 (m, 2H, ArH), 7.59–7.54 (m, 2H, ArH), 3.75 (s, 3H, OCH$_3$), 1.32 (s, 9H, *t*-BuH)

¹³C NMR: (151 MHz, DMSO-d_6) δ 165.94, 164.92, 155.56, 145.99, 145.16, 139.70, 138.39, 130.14, 127.99, 125.38, 52.33, 34.78, 30.85

Elemental analysis:

Theoretical: C, 65.16; H, 6.11; N, 13.41

Experimental: C, 64.79; H, 5.90; N, 13.72

IR (ATR-Ge, cm⁻¹): 3298, 2965, 1692(C=O), 1578, 1489, 1443, 1410, 1080

Compound 9

Chemical structure:
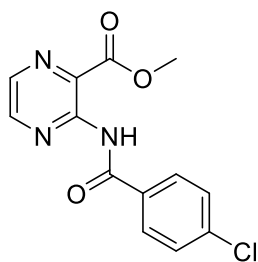
Laboratory Code: 4-Cl E

Chemical name: Methyl 3-(4-Chlorobenzamido)pyrazine-2-carboxylate

Chemical Formula: $C_{13}H_{10}ClN_3O_3$

Molecular weight: 291.04 g/mol

*Yield: 82%; 239 mg

Appearance: Beige solid

m.p.: 172.7–174.9 °C

^{1}H NMR: (500 MHz, CDCl$_3$) δ 11.72 (s, 1H, NHCO), 8.71 (d, J = 2.3 Hz, 1H. PzH), 8.45 (d, J = 2.3 Hz, 1H, PzH), 8.02–7.97 (m, 2H, ArH), 7.53–7.49 (m, 2H, ArH), 4.09 (s, 3H, OCH$_3$)

^{13}C NMR: (126 MHz, CDCl$_3$) δ 167.04, 163.35, 150.12, 147.14, 139.09, 138.60, 132.33, 129.22, 129.02, 128.64, 53.77

Elemental analysis:

Theoretical: C, 53.53; H, 3.46; N, 14.41

Experimental: C, 53.84; H, 3.36; N, 14.26

IR (ATR-Ge, cm^{-1}): 3206, 2957, 1702(C=O, CONH), 1684, 1596, 1509, 1486, 1455, 1129

Compound 10

Chemical structure:
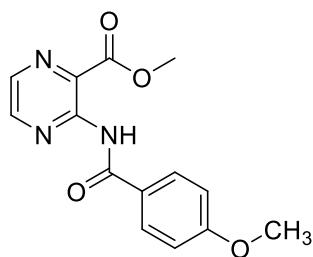
Laboratory Code: 4-MeO E

Chemical name: Methyl 3-(4-methoxybenzamido)pyrazine-2-carboxylate

Chemical Formula: $C_{14}H_{13}N_3O_4$

Molecular weight: 287.28 g/mol

*Yield: 82%; 236 mg

Appearance: White solid

m.p.: 144.5–145.0 °C

^{1}H NMR: (500 MHz, DMSO-d_6) δ 11.23 (s, 1H, NHCO), 8.70 (d, J = 2.4 Hz, 1H, PzH), 8.53 (d, J = 2.4 Hz, 1H, PzH), 8.06–7.99 (m, 2H, ArH), 7.11–7.05 (m, 2H, ArH), 3.85 (s, 3H, OCH$_3$), 3.74 (s, 3H, OCH$_3$).

^{13}C NMR: (126 MHz, DMSO-d_6) δ 165.46, 164.93, 162.68, 146.11, 145.10, 139.52, 138.38, 130.20, 124.90, 113.83, 55.51, 52.28.

Elemental analysis:

Theoretical: C, 58.53; H, 4.56; N, 14.63

Experimental: C, 58.00; H, 4.29; N, 14.09

IR (ATR-Ge, cm^{-1}): 3307, 1704 (C=O, CONH), 1607, 1496, 1443, 1127

Compound 11

Chemical structure:
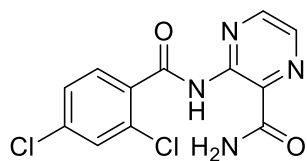
Laboratory Code: 2,4-diCl NH$_2$

Chemical Name: 3-(2,4-dichlorobenzamido)pyrazine-2-carboxamide

Chemical Formula: C$_{12}$H$_8$Cl$_2$N$_4$O$_2$

Molecular weight: 311.12 g/mol

*Yield: 76%; 236 mg

Appearance: white, solid

m.p.: 226–229°C

^{1}H NMR: (600 MHz, DMSO-d_6) δ 12.24 (s, 1H, NHCO), 8.56 (s, 1H, CONH), 8.55 (d, J = 2.4 Hz, 1H, PzH), 8.43 (d, J = 2.4 Hz, 1H, PzH), 8.12 (s, 1H, CONH), 7.76 (d, J = 2.0 Hz, 1H, ArH), 7.70–7.67 (m, 1H, ArH), 7.58 (dd, J = 8.3, 2.0 Hz, 1H, ArH).

^{13}C NMR: (151 MHz, DMSO-d_6) δ 163.69, 159.63, 157.55, 154.34, 151.01, 144.72, 131.18, 130.72, 121.45, 114.71, 55.69.

Elemental analysis:

Theoretical: C, 46.33; H, 2.59; N, 18.01

Experimental: C, 46.33; H, 2.68; N, 18.09

IR (ATR-Ge, cm^{-1}): 3392, 3196 (NH2), 1705 (C=O, CONH), 1646, 1622, 1542, 1507, 1120

Compound 12

Chemical structure:
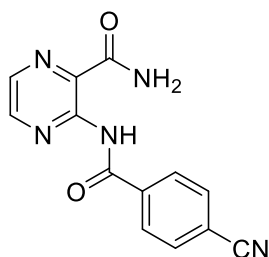
Laboratory Code: 4CN NH_2

Chemical Name: 3-(4-cyanobenzamido)pyrazine-2-carboxamide

Chemical Formula: $C_{13}H_9N_5O_2$

Molecular weight: 267.08 g/mol

*Yield: 69%; 184 mg

Appearance: White, solid

m.p.: 320 °C (carbonation)

¹H NMR: (600 MHz, DMSO-d_6) δ 12.88 (s, 1H, NHCO), 8.68 (d, J = 2.4 Hz, 1H, PzH), 8.63 (s, 1H, CONH), 8.46 (d, J = 2.4 Hz, 1H, PzH), 8.18 (s, 1H, CONH), 8.12–8.04 (m, 4H, ArH).

¹³C NMR: (151 MHz, DMSO-d_6) δ 168.48, 163.05, 148.90, 146.48, 138.94, 138.75, 133.47, 132.44, 129.65, 128.67, 118.56, 115.23

Elemental analysis:

Theoretical: C, 58.43; H, 3.39; N, 26.21

Experimental: C, 57.72; H, 3.43; N, 25.46

IR (ATR-Ge, cm⁻¹): 3368, 3198, 2239 (CN), 1681 (C=O, CONH), 1601, 1516, 1494, 1188

Compound 13

Chemical structure:
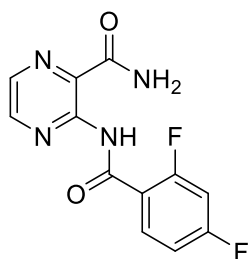
Laboratory Code: 2,4F NH_2

Chemical Name: 3-(2,4-difluorobenzamido)pyrazine-2-carboxamide

Chemical Formula: $C_{12}H_8F_2N_4O_2$

Molecular weight: 278.22 g/mol

*Yield: 77%; 214 mg

Appearance: Brown Solid

m.p.: 180 °C (Carbonation)

^{1}H NMR: (500 MHz, DMSO-d_6) δ 12.49 (s, 1H, NHCO), 8.64 (d, J = 2.4 Hz, 1H, PzH), 8.57 (s, 1H, CONH), 8.44 (d, J = 2.4 Hz, 1H, PzH), 8.12 (s, 1H, CONH), 7.94 (td, J = 8.7, 6.6 Hz, 1H, ArH), 7.70–7.37 (m, 1H, ArH), 7.28 (tdd, J = 8.9, 2.5, 0.8 Hz, 1H, ArH)

^{13}C NMR: (126 MHz, DMSO-d_6) δ 167.51, 164.12 (dd, J = 252.4, 12.5 Hz), 159.93 (dd, J = 253.3, 13.0 Hz), 159.90 (d, J = 2.1 Hz), 147.91, 145.63, 137.99, 132.51 (dd, J = 10.6, 3.7 Hz), 131.30, 120.80 – 119.15 (m), 112.32 (dd, J = 21.7, 3.6 Hz), 104.86 (t, J = 26.6 Hz)

Elemental analysis:

Theoretical: C, 51.81; H, 2.90; F, 13.66; N, 20.14; O, 11.50

IR: Not determined

HPLC: 99.93% Purity, 5% to 70% ACN/water gradient method.

Compound 14

Chemical structure:
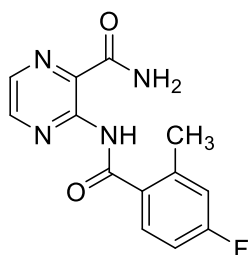
Laboratory Code: 2Me, 4F NH$_2$

Chemical Name: 3-(4-fluoro-2-methylbenzamido)pyrazine-2-carboxamide

Chemical Formula: C$_{13}$H$_{11}$FN$_4$O$_2$

Molecular weight: 274.26 g/mol

*Yield: 79%; 217 mg

Appearance: Beige Solid

m.p.: 219.1–220.9 °C

^{1}H NMR: (600 MHz, DMSO-d_6) δ 12.18 (s, 1H, NHCO), 8.62 (d, J = 2.4 Hz, 1H, PzH), 8.52 (s, 1H, CONH), 8.42 (d, J = 2.4 Hz, 1H, PzH), 8.07 (s, 1H, CONH), 7.68 (dd, J = 8.5, 5.9 Hz, 1H, ArH), 7.24–7.14 (m, 2H, ArH), 2.46 (s, 3H, Me).

^{13}C NMR: (151 MHz, DMSO-d_6) δ 167.79, 165.44, 162.86 (d, J = 247.8 Hz), 148.17, 145.74, 140.17 (d, J = 8.6 Hz), 137.92, 132.38 (d, J = 3.0 Hz), 132.10, 129.77 (d, J = 9.3 Hz), 117.82 (d, J = 21.5 Hz), 112.82 (d, J = 21.5 Hz), 19.63

Elemental analysis:

Theoretical: C, 56.93; H, 4.04; F, 6.93; N, 20.43; O, 11.67

IR: Not determined

HPLC: 98.60% purity, 5% to70% ACN/water gradient method.

3. RESULTS AND DISCUSSION

3.1. Chemistry

General scheme
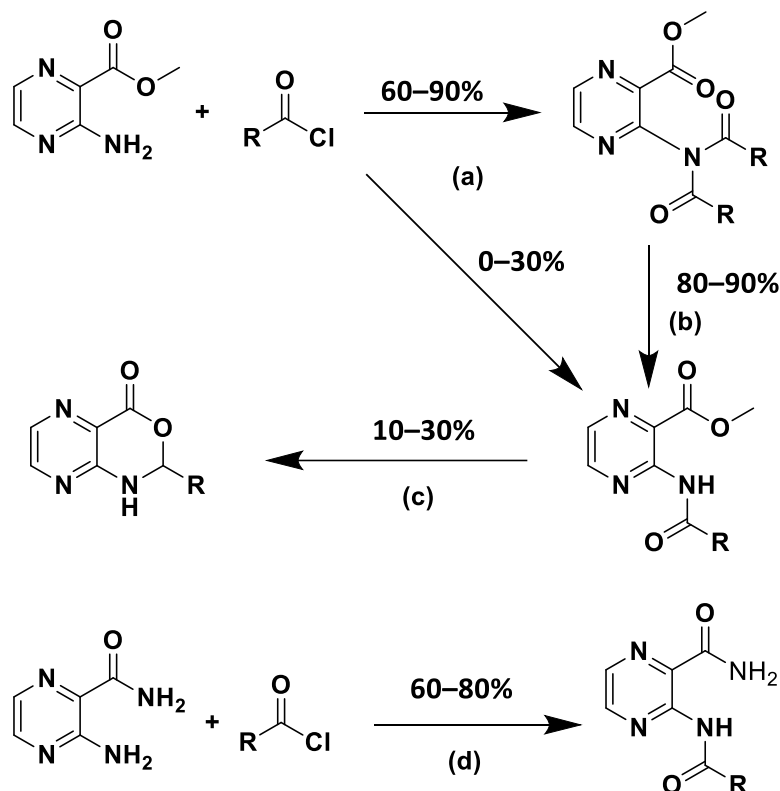
Scheme 5. General reaction procedure for synthesis of final compound.
(a) ACN solvent; Pyridine as Base; 70 °C; 24 h
(b) Hydrazine hydrate; THF solvent; Isopropanol as catalyst; Reflux for 1 h
(c) Anhyd. Toluene as solvent; triethylamine as base; 80 °C up to 6 h;
triphenylphosphine; 1,2-dibromotetrachloroethane
(d) ACN solvent; Pyridine as Base; 50 °C; 24 h

Synthesis of intermediate pyrazine carboxylate involves acylation of starting material (methyl 3-aminopyrazine-2-carboxylate) with various substituted benzoyl chlorides. The preparation of intermediate ester was a challenging step due to low reactivity of starting material at ambient temperature. Therefore, low reactivity and incomplete consumption of starting material during the reaction led to subsequent presence of traces of starting material in the acylated product. Thus, the separation of the desired product was also problematic due to similar retention factors between the starting material and the desired product. Increasing the temperature was a solution to achieve higher reactivity. However, by increasing the reactivity, a higher yield of diacylated side product was obtained in comparison to monoacylated product. However, monoacylated

product was the intermediate compound of interest for the synthesis of target compounds. Thus, following purification by flash chromatography, an additional step of reduction reaction in the presence of hydrazine hydrate in THF as solvent was involved for the preparation of monoacylated intermediate from diacylated products. Synthesis of diacylated product using procedure B solves the problem with the purification step using chromatographic methods since the difference in retention factors is considerably higher than in procedure A. Moreover, after all purification steps, the yield of monoacylated product obtained from the reduction reaction in procedure B (80–90%) was substantially increased compared to the yield obtained from procedure A (0–30%).

Cyclization of monoacylated intermediate was achieved with procedure C during which triphenylphosphine and 1,2-dibromotetrachloroethane reacted with intermediate ester as starting material in the triethylamine as base and anhyd. toluene as a solvent, under high temperature up to 80 °C. After complete reaction, residues of triethylammonium chloride were removed by filtration. Following evaporation of solvent, which was used during the reaction, the solid precipitate was obtained. Eventually, the solid precipitate was purified by recrystallization in ACN and gave 10–30% yield of final product.

Synthesis of final amide derivatives involved acylation of 3-aminopyrazine-2-carboxamide with substituted benzoyl chlorides at 50 ˚C; unlike the earlier acylation step, this reaction favors the monoacylated final products. We suppose that the observed tendency for monoacylation was mainly caused by the lower reaction temperature (50 ˚C vs previously used 70 ˚C). The increased reactivity of the 3-aminopyrazine-2-carboxamide towards acylation might be also connected with decreased steric hindrance – with unsubstituted carboxamidic moiety being less bulky in comparison with the methyl carboxylate moiety.

3.2. Biological Evaluation

Compound 1 to 5   Compound 6 to 10   Compound 11 to 14
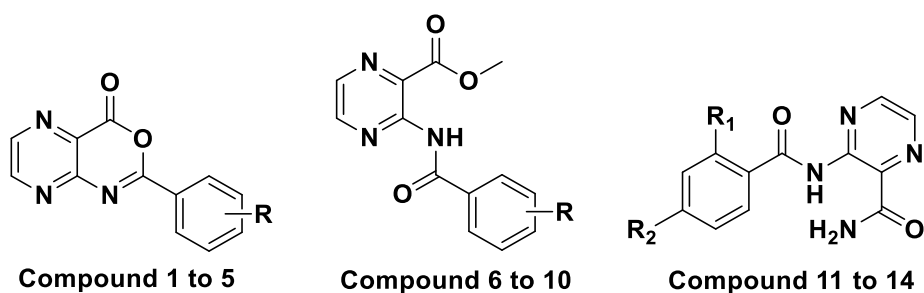
Table 2. Summarized antimycobacterial activity of compounds **1-14**.

Code	R/R₁	R₂	*M. smegmatis* MIC (μg/mL)	*M. aurum* MIC (μg/mL)	*M. avium* MIC (μg/mL)	*M. Kansasii* MIC (μg/mL)	*Mtb* H37Ra MIC (μg/mL)
1	4-Me	_	≥125	≥125	≥125	125	≥125
2	4-Cl	_	≥125	≥125	≥125	62.5	≥125
3	4-*tert*-Bu	_	250	250	≥500	≥500	≥500
4	4-MeO	_	≥500	≥500	≥500	≥500	≥500
5	2-F	_	≥500	≥500	≥500	≥500	≥500
6	4-Me	_	62.5	250	250	N.D.	N.D.
7	2-F	_	≥500	≥500	N.D.	N.D.	250
8	4-*tert*-Bu	_	N.D.	N.D.	N.D.	N.D.	N.D.
9	4-Cl	_	N.D.	N.D.	N.D.	N.D.	N.D.
10	4-MeO	_	≥500	≥500	N.D.	N.D.	250
11	2-Cl	4-Cl	500	≥500	250	62.5	≥500
12	_	4-CN	≥125	≥125	≥125	≥125	≥125
13	2-Me	4-F	N.D.	N.D.	N.D.	N.D.	N.D.
14	2-F	4-F	N.D.	N.D.	N.D.	N.D.	N.D.
INH	_	_	12.5	0.39	1000	6.25	0.25
RIF	_	_	0.125	0.015625	0.78	0.25	0.25

INH - isoniazid; RIF – rifampicin; N.D. - not determined

In total, seven final compounds were tested against five mycobacterial strains, and three out of five intermediate esters were previously studied and tested against three mycobacterial strains including virulent strains in Vinod Pallabotula et al.[3] Among five cyclized derivatives (pyrazine-oxazinone), compounds **1**, **2**, and **3** possess mild to moderate antimycobacterial activity. Compound **2** with chlorine substituent at position 4' has shown moderate antimycobacterial activity specifically against *M. kansasii* at MIC = 62.5 µg/mL. Moreover compound **1** with methyl substituent at position 4' has also shown some mild antimycobacterial activity against the same mycobacterial strain however at MIC = 125 µg/mL, two times higher than compound **2**. Compound **3** with t-butyl substituent at position 4' has shown mild activity against *M.aurum* and *M. smegmatis* strains at MIC = 250 µg/mL. However, in contrast to compounds **1** and **2**, no activity has been observed against *M. kansasii* and other mycobacterial strains. Cyclized derivatives (pyrazine-oxazinone) with substitution at position 4' with short alkyl particularly methyl or a higher homolog such as t-butyl and halogen have shown mild to moderate antimycobacterial activity in contrast to their precursors, intermediate methyl esters which were totally inactive. Currently, available experimental data from biological studies demonstrate the importance of substitution at position 4' with short alkyl or/and halogen for antimycobacterial activity as it was previously described by previously published articles.[3] All cyclized derivatives will be further subjected to testing for in-vitro metabolic studies for evaluation of prodrug activity in the biological environment. Furthermore, another series of compounds with carboxamide moiety were also prepared, among carboxamide derivatives, two compounds were subjected to biological testing. According to outcomes, compound **11** with Cl substitution at position 2' and concomitantly 4', has shown moderate activity against *M. kansasii* at MIC = 62.5 µg/mL. Moreover, mild activity has also been observed against *M. avium* at MIC = 250 µg/mL. Whereas in the case of compound **12** possessing CN moiety at position 4', no significant activity has been observed at measured concentration (MIC = 125 µg/mL) against any mycobacterial strains. Higher concentrations were not possible to measure due to precipitation. The importance of substitution at position 4' with halogen particularly Cl has been clearly demonstrated by the interpretation of currently available experimental data and results from biological studies hand in hand with a recently published article. As it was mentioned earlier in the above section for Derivatives of 3-amino-PZA as inhibitors of ProRS, one of their best compounds which has been recently synthesized and biologically tested against mycobacterial strains possess a Cl substitution at position 4'. This latter compound showed activity against *M. smegmatis* and the reference virulent strain *M.tuberculosis* H37Rv at MIC = 3.91 µg/mL. However, the activity has been lost significantly in the case of Cl substitution at

position 2' in the same series of previously published compounds.[3] This could justify the significance of halogen substitution, especially at position 4' of phenyl ring for compounds possessing antimycobacterial activity. As it was previously described in the section Derivatives of 3-amino-PZA as inhibitors of ProRS, the role of second position substituent is to improve binding affinity in hsProRs according to recent available studies.[4] Therefore, the synthesis of compound **11** with Cl substitution at positions 2' and 4' was an attempt to improve binding affinity to the enzyme mtProRS while concomitantly maintaining the antimycobacterial activity. However, in this case, no activity has been observed against *M. smegmatis* and the reference virulent strain *M. tuberculosis* H37Rv in contrast to the recently synthesized compound by our research group with a single Cl substituent at position 4'. Unlike compound **13** of a previously published article with a single Cl substituent at position 2' of the phenyl ring, which was completely inactive, mild to moderate activity was observed against *M. avium and M. kansasii* in the case of compound **11** with 2,4-diCl substituent.[52] Currently, available biological data and recent experimental studies brings us to the conclusion that overall antimycobacterial activity has lost significantly in comparison to previously synthesized carboxamide derivatives possessing Cl substituent solely at position 4'. However higher anti mycobacterial activity was observed compared to intermediate methyl esters which were almost completely inactive.[3]

3.3. *In silico* Studies

Database of 48 compounds including cyclized (pyrazine-oxazinone), carboxylic acids, methyl esters, and carboxamide derivatives were prepared manually for docking to mtProRS using ChemDraw software. All the prepared ligands share a 3-aminopyrazinamide core as a common structural feature. Ligands were drawn manually in ChemDraw, entitled by their codes, and SMILES were generated. The generated text file with SMILES was imported into MOE software and the ligands were prepared using a typical workflow. The dominant protomers were generated at pH 7, and 3D structures were rebuilt and minimized by employing the Wash utility in MOE.

The prepared database of ligands was docked into already prepared protein particularly ProRS of *M. tuberculosis* (mtProRS). Three-dimensional coordinates of mycobacterial prolyl-tRNA synthetase (mtProRS) were downloaded from the AlphaFold database (UniProt ID: P9WFT9).[54] Since The crystallographic structure of mtProRS (UniProt ID: P9WFT9) is not available, thus, a homology model constructed by AlphaFold-an artificial intelligence system developed by DeepMind was used. The main template used to build the model was a bacterial ProRS from *Enterococcus faecalis* (pdb id: 2J3L). The overlay of the two structures was used to manipulate proline (Pro) and adenosine as a substrate and a substrate-like compound, respectively, into the homology model. The rotamer of Thr111 sidechain was changed to match the conformation of the corresponding Thr in the template (necessary for the interaction with Pro substrate). Additionally, the water molecule forming the water bridge between adenosine N-3 and Ser461 as seen in EfProRS (pdb id: 2J3L). This water bridge often occurs also in other crystallographic structures of ProRS and participates in the interactions. The importance of this water molecule was previously confirmed by the Solvent Analysis application using the 3D-RISM model.[55] For this reason, water molecule crystallography was kept in the receptor for docking. Proline was set as a part of the receptor. The pocket was defined as a set of residues with at least one atom within 4.5 Å from the overlayed ligand (adenosine). The resulting system (mtProRS homology model with Pro, adenosine, one molecule of water, and manipulated Thr111) was prepared by MOE QuickPrep functionality with default settings, which included corrections of structural errors, the addition of hydrogens, calculation of partial charges, 3D optimization of protonation/tautomeric states and H-bond network (Protonate3D) and a restrained minimization (to RMS gradient of 0.01 kcal.mol^{-1}. Å^{-1}. In previous studies, the binding of similar 3-aminopyrazinamide derivatives to hsProRS was found to be Pro-

dependent. For this reason, the pocket for docking was determined by the position of the adenosine, and our compounds were docked alongside the Pro substrate.[3]

Prepared ligands were docked to mtProRS. Ligands were treated as flexible, and all rotatable bonds were allowed to rotate whereas the receptor was treated as rigid by applying the following (predefined) settings of the docking protocol: Placement> Triangle Matcher, London dG, 30 poses Refinement> Rigid Receptor, GBVI/WSA dG, 5 poses. As an outcome of docking, a large database of ligands' poses was generated with different docking scores. The ligand-target binding affinity was estimated based on the GBVI/WSA scoring function.[3] A more negative value means higher binding affinity to the target since the energy is released upon binding of the ligand to the receptor. The resulting database of ligands' poses was further optimized by applying PLIF (Protein-Ligand Interaction Fingerprints) analysis implemented in MOE, through which the most relevant interactions with specific amino acid residues were selected. The significance of H-bond interactions with Ala154 and Arg142 was previously demonstrated by available experimental data.[3] Thus poses with interaction to Ala154 and also Arg142 were selected for further analysis. Following PLIF analysis, in total 22 ligands (out of 48) were found to exert the desired interactions - 12 cyclized (pyrazine-oxazinone) derivatives (**11-22**) and 10 carboxamide derivatives (**1-10**) were subjected to further evaluation, see **Table 3**. Esters and carboxylic acid derivatives were not present among the final database of 22 ligands as they have been excluded earlier via the scoring function and the lack of the key intended interactions.

VIRTUAL LIBRARY
OF COMPOUNDS
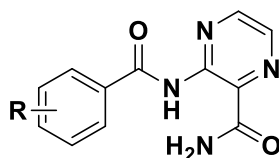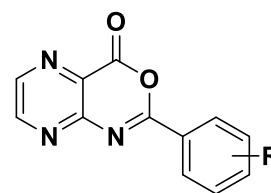
Compounds V1 to V10   Compounds V11 - V22

Table 3. Summarized docking results into mtProRS based on interactions and scoring function of virtual compounds (V**1-V22).**

Virtual No.	Synthesized as	R	Arg142	Ala154	π-π interaction	Additional interactions	Score
V1	-	2-F	+	+	-	-	-7.27
V2	-	2-Cl	+	+	-	-	-7.08
V3	-	2-Me	+	+	+	-	-7.03
V4	-	4-Me	+	+	-	-	-6.63
V5	-	4-Cl	+	+	-	-	-6.60
V6	-	4-*tert*-Bu	-	+	-	Arg462 HBD with N atom in pyrazine ring HBA	-6.60
V7	**Compound 12**	4-CN	+	+	+	-	-6.59
V8	-	4-MeO	+	+	-	-	-6.45
V9	-	2,4-diMe	+	+	-	-	-6.45
V10	-	3-Cl	+	+	+	-	-6.37
V11	-	3-Me	+	+	+	-	-7.16
V12	-	2-Me	+	+	+	Arg462 HBD with C=O HBA	-6.98
V13	-	3-Cl	+	+	+	-	-6.97
V14	**Compound 5**	2-F	+	+	-	Arg462 HBD with C=O HBA	-6.95
V15	**Compound 1**	4-Me	+	-	+	-	-6.90
V16	**Compound 4**	4-MeO	-	-	-	Arg462 HBD with C=O HBA	-6.87
V17	**Compound 2**	4-Cl	+	+	+	-	-6.83

V18	-	2,4-diMe	+	-	-	Arg462 HBD with C=O HBA	-6.75
V19	-	2-Cl	+	+	+	Arg462 HBD with C=O HBA	-6.70
V20	**Compound 3**	4-*tert*-Bu	arene-cation interaction	-	-	Gly424 HBD with N atom in pyrazine ring HBA	-6.60
V21	-	2-Cl, 4-CN	-	-	-	Arg462 HBD with C=O HBA	-6.56
V22	-	2,4-diCl	-	-	-	1-Glu144 HBA with 4-Cl 2-Arg462 HBD with C=O	-6.53

Among carboxamide derivatives (**V1-V10**), compound **V1** with F substituent at position 2' of the benzene ring, which has been previously studied by our research group,[3] possesses the best binding score. Moreover, the representative binding mode of compound **V1** was fully consistent with adenosine as the original ligand. (refer to Figure 10 and Figure 11). In Figure 10, the position of the adenosine substrate-like fragment is taken from the reference.[3]
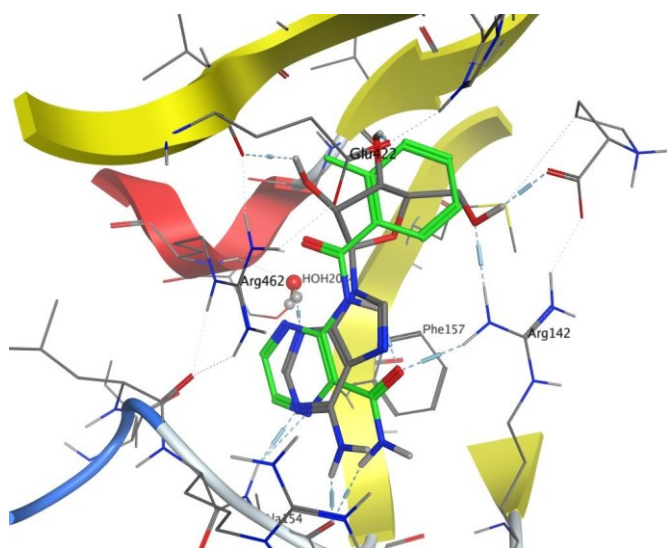
Figure 10. 3-(2-Fluorobenzamido)pyrazine-2-carboxamide (**V1**, green carbons) docked into mtProRS in comparison with adenosine (grey carbons).
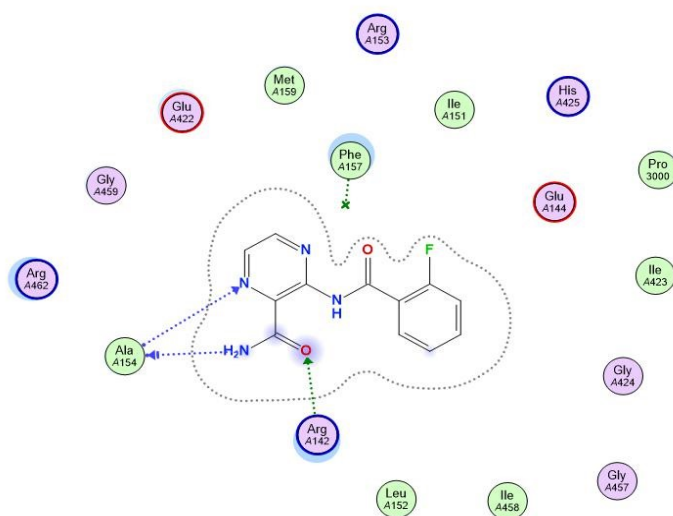
Figure 11. 2D ligand interaction diagram of 3-(2-fluorobenzamido)pyrazine-2-carboxamide (**V1**) docked to mtProRS.

Compound **V7** (newly synthesized as **Compound 12**) with 4'-CN moiety possessed the expected binding mode and also the same type of interactions with Ala154, Arg142, and π-π interaction between pyrazine core and Phe157 (refer to Figure 12).
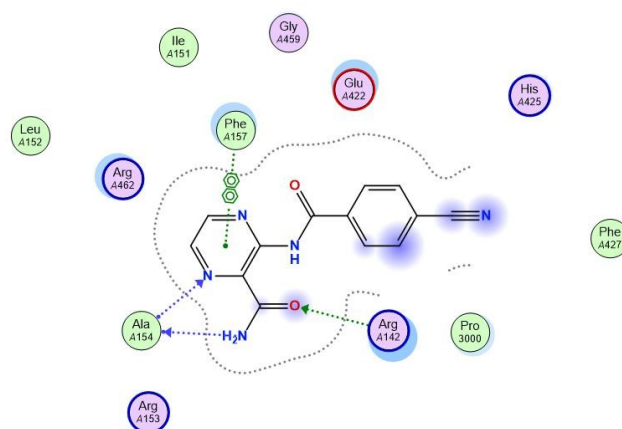
Figure 12. 2D ligand interaction diagram of 3-(4-cyanobenzamido)pyrazine-2-carboxamide (V**7, Compound 12**) docked to mtProRS.

In all carboxamide derivatives (**V1-V10**), an H-bond interaction has been observed between the carbonyl group of carboxamide moiety (acceptor) and Arg142 side chain (donor). Moreover, another H-bond interaction has been observed between the amino group of carboxamide moiety

(donor) and Ala154 backbone (acceptor) and a similar interaction has occurred between the N-1 atom present in pyrazine ring (acceptor) and Ala154 sidechain (donor). In several compounds π-π interactions have been observed between pyrazine core and Phe157.

Among cyclized derivatives (pyrazine-oxazines), the best score belongs to compound **V11** with 3'-CH$_3$, Compound **V11** possesses H-bond interaction with Ala154 and Arg142. Additionally, π-π interaction was observed with Phe157 which is depicted in Figure 13 and Figure 14. Despite the same interacting amino acid residues, the binding mode of the cyclized derivatives (**V11-V22)** is significantly different from the binding mode of the carboxamides and adenosine as the original ligand.
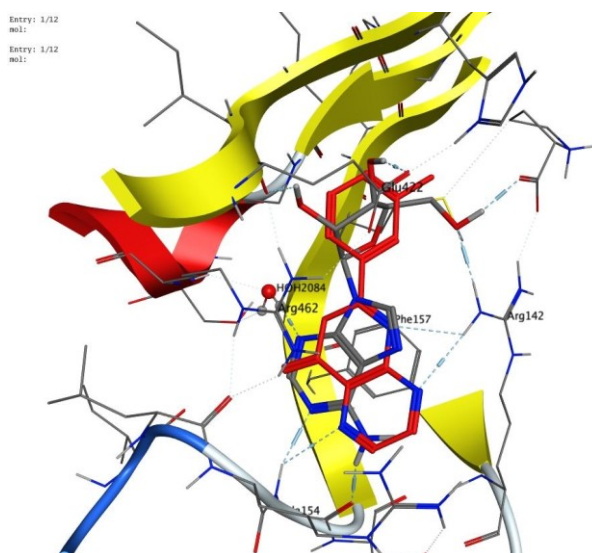
Figure 13. 2-(*m*-tolyl)-4*H*-pyrazino[2,3-*d*][1,3]oxazin-4-one (**V11**, red carbons) docked into mtProRS in comparison with adenosine (grey carbons).
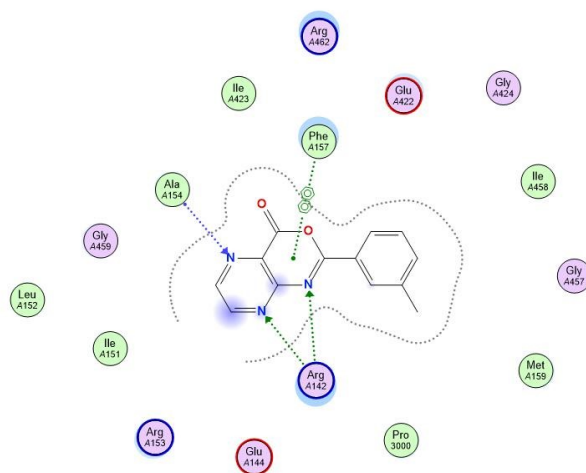
Figure 14. 2D ligand interaction diagram of [2-(*m*-tolyl)-4H-pyrazino[2,3-*d*][1,3]oxazin-4-one] (**V11**) docked to mtProRS.

Almost all cyclized derivatives (pyrazine-oxazinone) possess strong H-bond interaction with Ala154 and/or Arg142 except for compound **V22** which possess a new interaction with Glu144 and Arg462. Interestingly the outcomes of this experiment were consistent with recently studied carboxamide derivatives by our research group.[3] Almost all cyclized derivatives bind to the same binding site as previously studied carboxamide derivatives however the binding mode is significantly different than previously published compounds.[3] Typically H-bond interactions have been observed between the N atom present in the pyrazine ring and Arg142. Moreover, in some derivatives, similar interaction occurs between adjacent nitrogen atoms present in the oxazinone ring and Arg142. Another interaction has been observed between the second nitrogen atom present in the pyrazine ring and Ala154. In some derivatives interaction between Phe157 and pyrazine core has been observed. Compound **V22** with Cl substituent at positions 2' and 4' possesses relatively new interaction with rather different aa sequence compared to previously studied carboxamide derivatives with Cl substituent at position 4'(refer to Figure 15).[3]
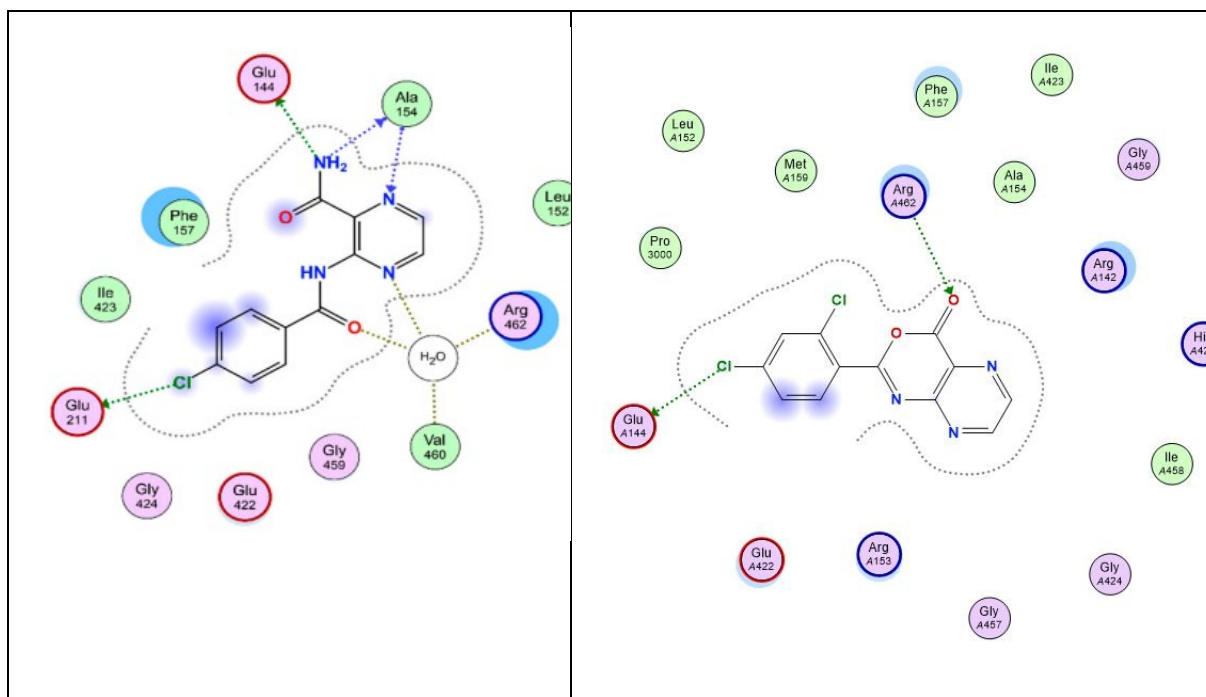
Figure 15. 2D ligand interaction diagram of (LEFT) the previously published 3-(4-chlorobenzamido)pyrazine-2-carboxamide; and (RIGHT) newly synthesized derivative 2-(2,4-dichlorophenyl)-4H-pyrazino[2,3-d][1,3]oxazin-4-one (**V22**), demonstrating a new interaction with mtProRS.

Methyl esters and carboxylic acid derivatives were excluded following PLIF analysis since they lack the expected binding mode to the enzyme as has been demonstrated by recently available studies. Whereas carboxamide derivatives bear the same binding mode as previously synthesized carboxamide derivatives with few exceptions (refer to Figure 16), we found that cyclized derivatives (pyrazine-oxazinone) could also bind to the enzyme mtProRS, but with a significantly different binding mode (refer to Figure 17), Therefore, novel in-silico studied compounds could potentially target mtProRS as well. Thus, these compounds could be promising candidates for future target studies and will be subjected to further evaluation against mtProRS once the protein is available.
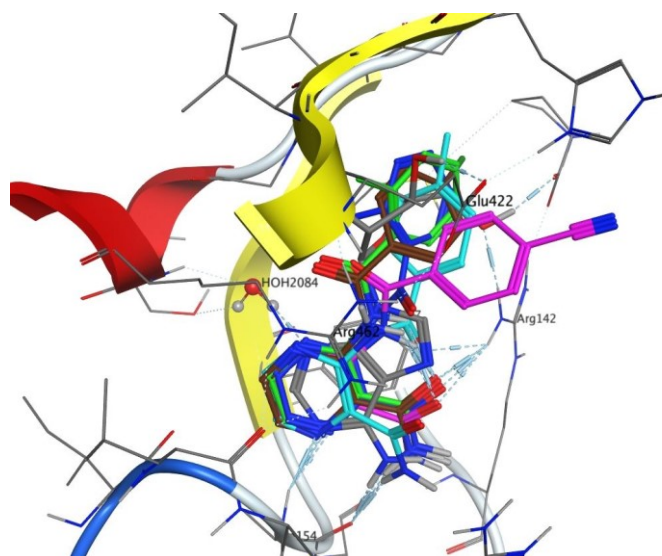
Figure 16. Binding mode of carboxamide derivatives (**V1**, **V3**, **V4**, **V5**, **V7)** depicted with (R=2-Me, blue carbons; R=2-F, green carbons; 4-Cl, brown; 4-Me arctic blue; 4-CN, bright purple) docked into mtProRS, in overlay with adenosine (grey carbons).
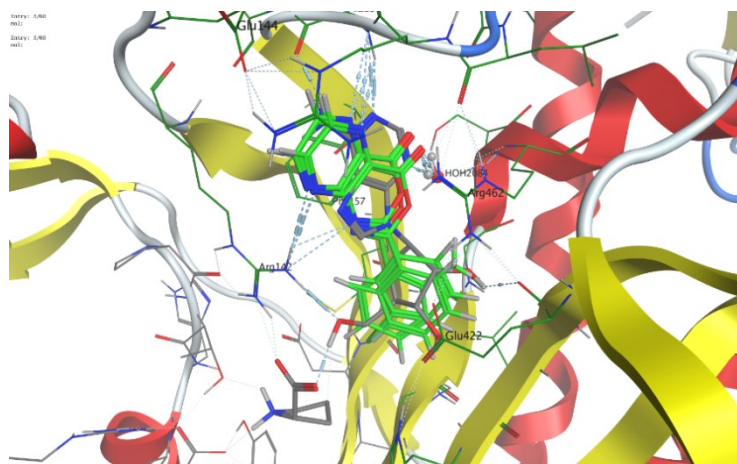
Figure 17. Binding mode of cyclized derivatives (**V11**, **V12**, **V13**, **V14)** - depicted with green carbons - (R=3-Me, 3-Cl, 2-F, 2-Me) and original adenosine ligand (grey carbons) docked to mtProRS.

4. CONCLUSION

To sum up this experiment, I have synthesized 14 compounds including cyclized derivatives, carboxamide derivatives, and methyl ester derivatives bearing pyrazine pharmacophore as common structural features. Out of 14 compounds, seven compounds including five cyclized derivatives (**1-5**) and two carboxamide derivatives (**11, 12**) were biologically tested and three out of five methyl ester derivatives (**6, 7, 10**) were previously studied and biologically evaluated by our research group. Cyclized derivatives (pyrazine-oxazinone) compound (**1, 2, 3**) with substitution at position 4' with short alkyl particularly methyl or a higher homolog such as *tert*-butyl and halogen have shown mild to moderate antimycobacterial activity in contrast to their precursors, intermediate methyl esters, which were totally inactive. Therefore, currently available results from biological studies could justify the importance of substitution at position 4' with short alkyl or/and halogen for antimycobacterial activity as it was previously demonstrated by our research group.[3] Among carboxamide derivatives, compound **11** (R = 2,4-diCl) has shown moderate antimycobacterial activity. Whereas in the case of compound **12** (R = 4-CN), no significant activity has been observed at measured concentration against any mycobacterial strains. The importance of substitution at position 4' with halogen particularly Cl has been clearly demonstrated by our research group.[3] One of their best compounds which has been recently synthesized and biologically tested against mycobacterial strains possesses a Cl substitution at position 4'. However, the activity has been lost significantly in the case of Cl substitution at position 2' in the same series of previously published compounds.[3] This could justify the significance of halogen substitution, especially at position 4' of the phenyl ring for compounds possessing antimycobacterial activity. The role of second position substituent is to improve binding affinity toward ProRS according to recent available studies. Therefore, synthesis of compound **11** with Cl disubstitution at positions 2' and 4' was an attempt to improve binding affinity to the enzyme mtProRS while concomitantly maintaining the antimycobacterial activity. However, in this case, the expectation were not fulfilled and the disubstitution led to a significant decrease of activity. Outcome of this experiment and recent available experimental studies bring us to the conclusion that overall antimycobacterial activity was lost to a significant extent in comparison to previously synthesized carboxamide derivatives possessing Cl substituent solely at position 4'. However higher antimycobacterial activity was observed compared to intermediate methyl esters which were almost completely inactive.[3]

Recently available studies reported the design and synthesis of 3-amino-POA analogs as inhibitors of mycobacterial aspartate decarboxylase (PanD).[1] Therefore, we hypothesized that

cyclized derivatives (pyrazine-oxazinone) can act as prodrugs which may get metabolically converted to POA derivatives upon exposure to the biological environment. Based on this hypothesis we designed and synthesized novel compounds which could potentially target the PanD of mycobacteria. All cyclized derivatives will be further subjected to testing for in-vitro metabolic studies for evaluation of prodrug activity in the organism/biological environment.

5. REFERENCES

(1) Ragunathan, P.; Cole, M.; Latka, C.; Aragaw, W. W.; Hegde, P.; Shin, J.; Subramanian Manimekalai, M. S.; Rishikesan, S.; Aldrich, C. C.; Dick, T. Mycobacterium tuberculosis PanD structure–function analysis and identification of a potent pyrazinoic acid-derived enzyme inhibitor. *ACS chemical biology* **2021**, *16* (6), 1030-1039.

(2) Adachi, R.; Okada, K.; Skene, R.; Ogawa, K.; Miwa, M.; Tsuchinaga, K.; Ohkubo, S.; Henta, T.; Kawamoto, T. Discovery of a novel prolyl-tRNA synthetase inhibitor and elucidation of its binding mode to the ATP site in complex with l-proline. *Biochem Biophys Res Commun* **2017**, *488* (2), 393-399. DOI: 10.1016/j.bbrc.2017.05.064 From NLM.

(3) Pallabothula, V. S. K.; Kerda, M.; Juhás, M.; Janďourek, O.; Konečná, K.; Bárta, P.; Paterová, P.; Zitko, J. Adenosine-Mimicking Derivatives of 3-Aminopyrazine-2-Carboxamide: Towards Inhibitors of Prolyl-tRNA Synthetase with Antimycobacterial Activity. *Biomolecules* **2022**, *12* (11), 1561.

(4) Pang, L.; Weeks, S. D.; Juhás, M.; Strelkov, S. V.; Zitko, J.; Van Aerschot, A. Towards Novel 3-Aminopyrazinamide-Based Prolyl-tRNA Synthetase Inhibitors: In Silico Modelling, Thermal Shift Assay and Structural Studies. *Int. J. Mol. Sci.* **2021**, *22* (15), 7793. DOI: 10.3390/ijms22157793.

(5) Ravimohan, S.; Kornfeld, H.; Weissman, D.; Bisson, G. P. Tuberculosis and lung damage: from epidemiology to pathophysiology. *European respiratory review* **2018**, *27* (147).

(6) Padda, I. S.; Reddy, K. M. Antitubercular medications. In *StatPearls [Internet]*, StatPearls Publishing, 2022.

(7) Kiazyk, S.; Ball, T. Tuberculosis (TB): Latent tuberculosis infection: An overview. *Canada Communicable Disease Report* **2017**, *43* (3-4), 62.

(8) Rodriguez-Takeuchi, S. Y.; Renjifo, M. E.; Medina, F. J. Extrapulmonary tuberculosis: pathophysiology and imaging findings. *Radiographics* **2019**, *39* (7), 2023-2037.

(9) Abu-Zidan, F. M.; Sheek-Hussein, M. Diagnosis of abdominal tuberculosis: lessons learned over 30 years: pectoral assay. *World Journal of Emergency Surgery* **2019**, *14* (1), 1-7.

(10) Méchaï, F.; Bouchaud, O. Tuberculous meningitis: challenges in diagnosis and management. *Revue neurologique* **2019**, *175* (7-8), 451-457.

(11) Alsayed, S. S.; Gunosewoyo, H. Tuberculosis: pathogenesis, current treatment regimens and new drug targets. *Int. J. Mol. Sci.* **2023**, *24* (6), 5202.

(12) Khawbung, J. L.; Nath, D.; Chakraborty, S. Drug resistant Tuberculosis: A review. *Comparative immunology, microbiology and infectious diseases* **2021**, *74*, 101574.

(13) Zha, B. S.; Nahid, P. Treatment of drug-susceptible tuberculosis. *Clinics in chest medicine* **2019**, *40* (4), 763-774.

(14) Umumararungu, T.; Mukazayire, M. J.; Mpenda, M.; Mukanyangezi, M. F.; Nkuranga, J. B.; Mukiza, J.; Olawode, E. O. A review of recent advances in anti-tubercular drug development. *indian journal of tuberculosis* **2020**, *67* (4), 539-559.

(15) Bahuguna, A.; Rawat, D. S. An overview of new antitubercular drugs, drug candidates, and their targets. *Medicinal research reviews* **2020**, *40* (1), 263-292.

(16) Lamont, E. A.; Dillon, N. A.; Baughn, A. D. The bewildering antitubercular action of pyrazinamide. *Microbiology and Molecular Biology Reviews* **2020**, *84* (2), 10.1128/mmbr. 00070-00019.

(17) Zhang, Y.; Shi, W.; Zhang, W.; Mitchison, D. Mechanisms of pyrazinamide action and resistance. *Microbiology spectrum* **2014**, *2* (4), 10.1128/microbiolspec. mgm1122-0023-2013.

(18) Rajendran, A.; Palaniyandi, K. Mutations associated with pyrazinamide resistance in Mycobacterium tuberculosis: a review and update. *Current Microbiology* **2022**, *79* (11), 348.

(19) Zhang, Y.; Scorpio, A.; Nikaido, H.; Sun, Z. Role of acid pH and deficient efflux of pyrazinoic acid in unique susceptibility of Mycobacterium tuberculosis to pyrazinamide. *Journal of bacteriology* **1999**, *181* (7), 2044-2049.

(20) Lamont, E. A.; Baughn, A. D. Impact of the host environment on the antitubercular action of pyrazinamide. *EBioMedicine* **2019**, *49*, 374-380.

(21) Gopal, P.; Grüber, G.; Dartois, V.; Dick, T. Pharmacological and molecular mechanisms behind the sterilizing activity of pyrazinamide. *Trends in pharmacological sciences* **2019**, *40* (12), 930-940.

(22) Adams, L. M.; Andrews, R. J.; Hu, Q. H.; Schmit, H. L.; Hati, S.; Bhattacharyya, S. Crowder-induced conformational ensemble shift in Escherichia coli Prolyl-tRNA synthetase. *Biophysical Journal* **2019**, *117* (7), 1269-1284.

(23) Hegde, P. V.; Aragaw, W. W.; Cole, M. S.; Jachak, G.; Ragunathan, P.; Sharma, S.; Harikishore, A.; Grüber, G.; Dick, T.; Aldrich, C. C. Structure activity relationship of pyrazinoic acid analogs as potential antimycobacterial agents. *Bioorganic & Medicinal Chemistry* **2022**, *74*, 117046.

(24) Yelamanchi, S. D.; Surolia, A. Targeting amino acid metabolism of Mycobacterium tuberculosis for developing inhibitors to curtail its survival. *IUBMB life* **2021**, *73* (4), 643-658.

(25) Monteiro, D. C.; Patel, V.; Bartlett, C. P.; Nozaki, S.; Grant, T. D.; Gowdy, J. A.; Thompson, G. S.; Kalverda, A. P.; Snell, E. H.; Niki, H. The structure of the PanD/PanZ protein complex reveals negative feedback regulation of pantothenate biosynthesis by coenzyme A. *Chemistry & biology* **2015**, *22* (4), 492-503.

(26) Shi, W.; Chen, J.; Feng, J.; Cui, P.; Zhang, S.; Weng, X.; Zhang, W.; Zhang, Y. Aspartate decarboxylase (PanD) as a new target of pyrazinamide in Mycobacterium tuberculosis. *Emerging microbes & infections* **2014**, *3* (1), 1-8.

(27) Sun, Q.; Li, X.; Perez, L. M.; Shi, W.; Zhang, Y.; Sacchettini, J. C. The molecular basis of pyrazinamide activity on Mycobacterium tuberculosis PanD. *Nature communications* **2020**, *11* (1), 339.

(28) Gopal, P.; Sarathy, J. P.; Yee, M.; Ragunathan, P.; Shin, J.; Bhushan, S.; Zhu, J.; Akopian, T.; Kandror, O.; Lim, T. K. Pyrazinamide triggers degradation of its target aspartate decarboxylase. *Nature communications* **2020**, *11* (1), 1661.

(29) Gopal, P.; Dick, T. Targeted protein degradation in antibacterial drug discovery? *Progress in biophysics and molecular biology* **2020**, *152*, 10-14.

(30) Xu, X.; Zhang, L.; Yang, T.; Qiu, Z.; Bai, L.; Luo, Y. Targeting caseinolytic protease P and its AAA1 chaperone for tuberculosis treatment. *Drug Discovery Today* **2023**, 103508.

(31) Hameed, H. A.; Tan, Y.; Islam, M. M.; Lu, Z.; Chhotaray, C.; Wang, S.; Liu, Z.; Fang, C.; Tan, S.; Yew, W. W. Detection of novel gene mutations associated with pyrazinamide resistance in multidrug-resistant Mycobacterium tuberculosis clinical isolates in Southern China. *Infection and Drug Resistance* **2020**, 217-227.

(32) Gopal, P.; Tasneen, R.; Yee, M.; Lanoix, J.-P.; Sarathy, J.; Rasic, G.; Li, L.; Dartois, V. r.; Nuermberger, E.; Dick, T. In vivo-selected pyrazinoic acid-resistant Mycobacterium

tuberculosis strains harbor missense mutations in the aspartate decarboxylase PanD and the unfoldase ClpC1. *ACS infectious diseases* **2017**, *3* (7), 492-501.

(33) Xie, S.; Griffin, M. D.; Winzeler, E. A.; Ribas de Pouplana, L.; Tilley, L. Targeting Aminoacyl tRNA Synthetases for Antimalarial Drug Development. *Annual Review of Microbiology* **2023**, *77*.

(34) Pang, L. P.; Weeks, S. D.; Van Aerschot, A. Aminoacyl-tRNA Synthetases as Valuable Targets for Antimicrobial Drug Discovery. *Int. J. Mol. Sci.* **2021**, *22* (4), 34, Review. DOI: 10.3390/ijms22041750.

(35) Bouz, G.; Zitko, J. Inhibitors of aminoacyl-tRNA synthetases as antimycobacterial compounds: An up-to-date review. *Bioorganic Chemistry* **2021**, *110*, 104806. DOI: 10.1016/j.bioorg.2021.104806.

(36) Ivanov, K.; Moor, N.; Lavrik, O. Non-canonical functions of aminoacyl-tRNA synthetases. *BIOCHEMISTRY C/C OF BIOKHIMIIA* **2000**, *65* (8), 888-897.

(37) Kim, S.-H.; Bae, S.; Song, M. Recent development of aminoacyl-tRNA synthetase inhibitors for human diseases: A future perspective. *Biomolecules* **2020**, *10* (12), 1625.

(38) Nasim, F.; Qureshi, I. A. Aminoacyl tRNA Synthetases: Implications of Structural Biology in Drug Development against Trypanosomatid Parasites. *ACS omega* **2023**, *8* (17), 14884-14899.

(39) Pena, N.; Dranow, D. M.; Hu, Y.; Escamilla, Y.; Bullard, J. M. Characterization and structure determination of prolyl-tRNA synthetase from Pseudomonas aeruginosa and development as a screening platform. *Protein Science* **2019**, *28* (4), 727-737.

(40) Travin, D. Y.; Severinov, K.; Dubiley, S. Natural Trojan horse inhibitors of aminoacyl-tRNA synthetases. *RSC Chemical Biology* **2021**, *2* (2), 468-485.

(41) Qiao, H.; Xia, M.; Cheng, Y.; Zhou, J.; Zheng, L.; Li, W.; Wang, J.; Fang, P. Tyrosine-targeted covalent inhibition of a tRNA synthetase aided by zinc ion. *Communications Biology* **2023**, *6* (1), 107.

(42) Volynets, G. P.; Usenko, M. O.; Gudzera, O. I.; Starosyla, S. A.; Balanda, A. O.; Syniugin, A. R.; Gorbatiuk, O. B.; Prykhod'ko, A. O.; Bdzhola, V. G.; Yarmoluk, S. M. Identification of dual-targeted Mycobacterium tuberculosis aminoacyl-tRNA synthetase inhibitors using machine learning. *Future Medicinal Chemistry* **2022**, *14* (17), 1223-1237.

(43) Hoffmann, G.; Le Gorrec, M.; Mestdach, E.; Cusack, S.; Salmon, L.; Jensen, M. R.; Palencia, A. Adenosine-Dependent Activation Mechanism of Prodrugs Targeting an Aminoacyl-tRNA Synthetase. *Journal of the American Chemical Society* **2023**, *145* (2), 800-810.

(44) Ho, J. M.; Bakkalbasi, E.; Söll, D.; Miller, C. A. Drugging tRNA aminoacylation. *RNA Biol* **2018**, *15* (4-5), 667-677. DOI: 10.1080/15476286.2018.1429879 From NLM.

(45) Sharma, N.; Sharma, D. An upcoming drug for onychomycosis: Tavaborole. *Journal of Pharmacology and Pharmacotherapeutics* **2015**, *6* (4), 236-239.
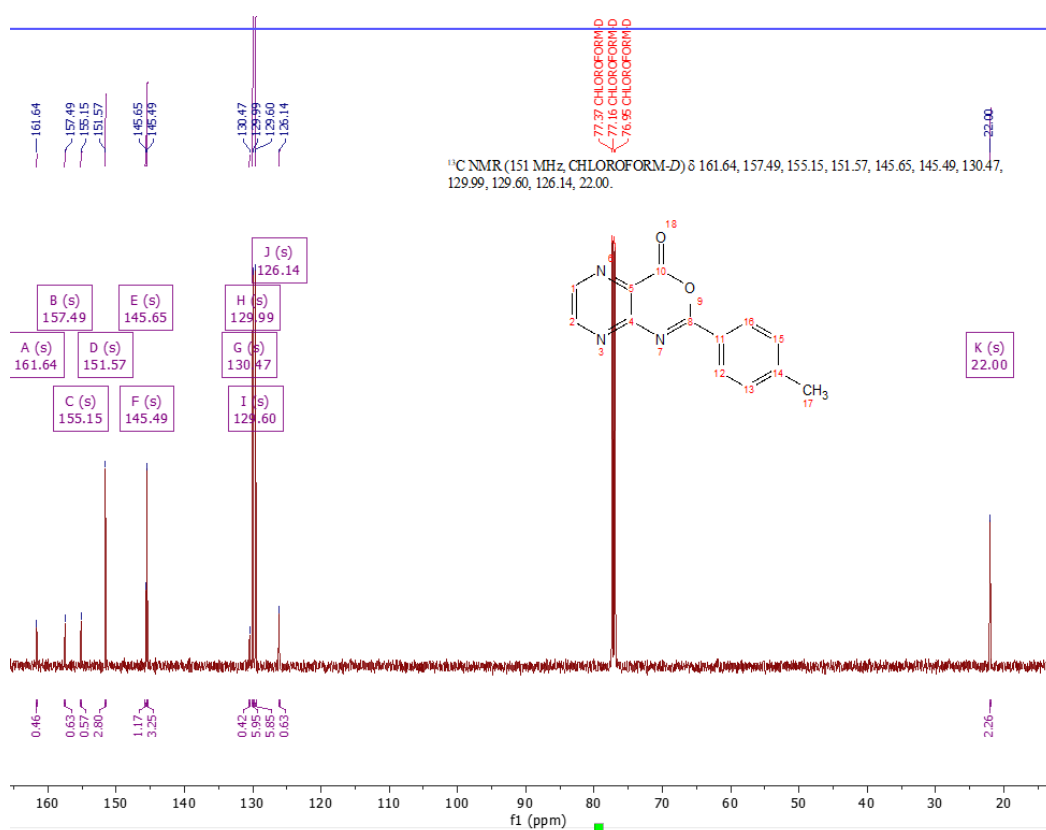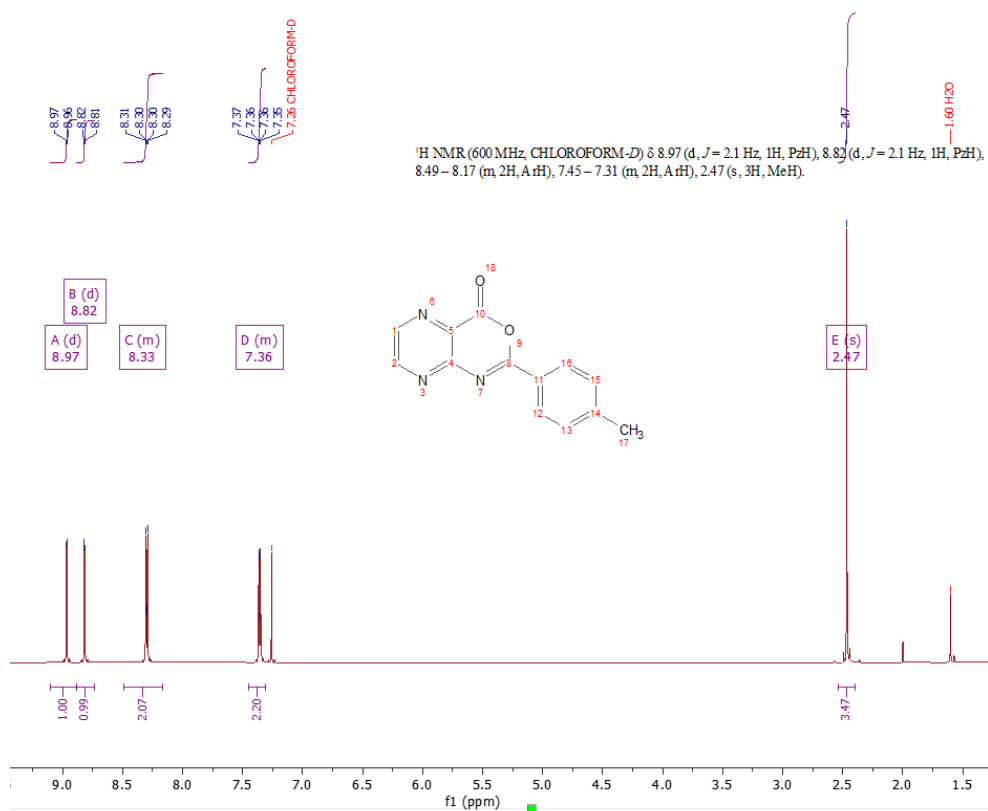
(46) Pines, M.; Spector, I. Halofuginone—the multifaceted molecule. *Molecules* **2015**, *20* (1), 573-594.

(47) Jain, P. P.; Zhao, T.; Xiong, M.; Song, S.; Lai, N.; Zheng, Q.; Chen, J.; Carr, S. G.; Babicheva, A.; Izadi, A. Halofuginone, a promising drug for treatment of pulmonary hypertension. *British journal of pharmacology* **2021**, *178* (17), 3373-3394.
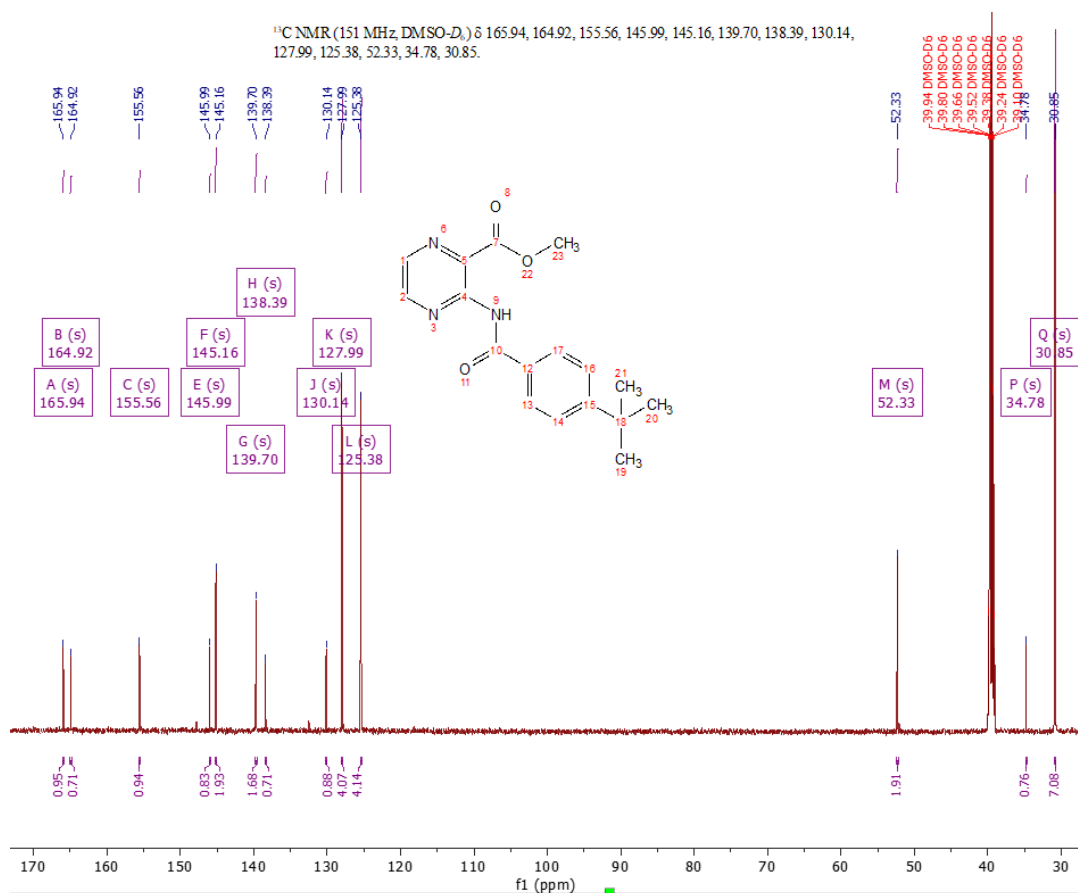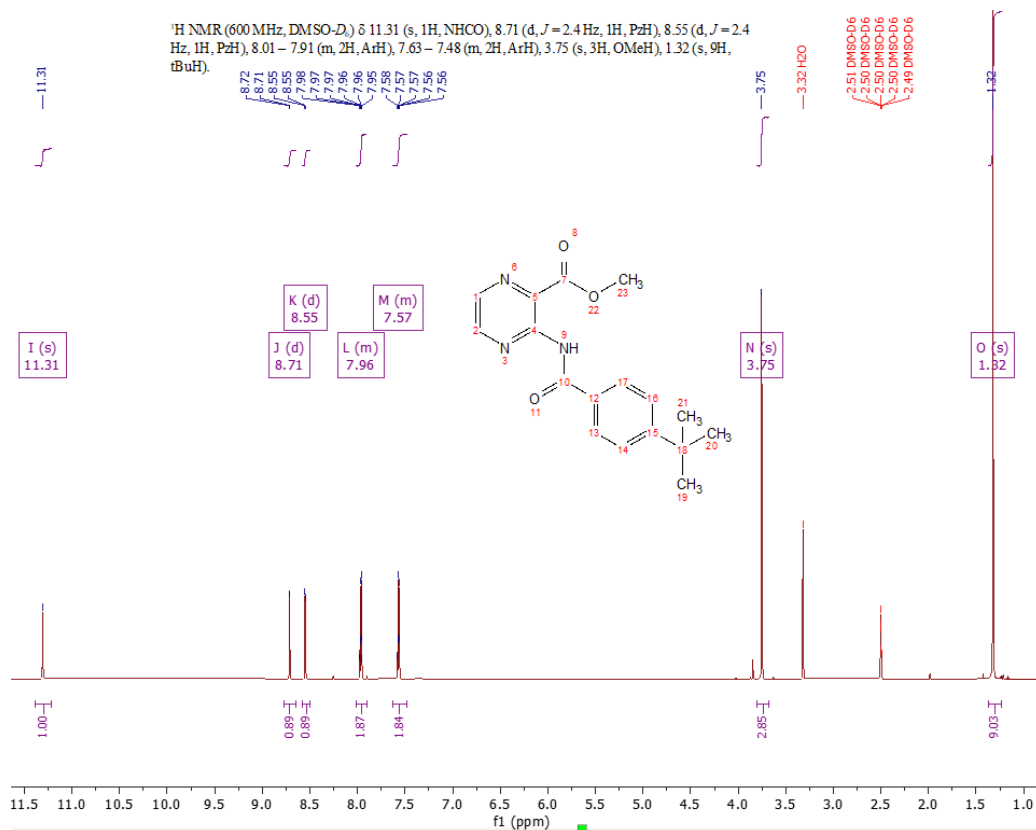
(48) Tye, M. A.; Payne, N. C.; Johansson, C.; Singh, K.; Santos, S. A.; Fagbami, L.; Pant, A.; Sylvester, K.; Luth, M. R.; Marques, S. Elucidating the path to Plasmodium prolyl-tRNA synthetase inhibitors that overcome halofuginone resistance. *Nature Communications* **2022**, *13* (1), 4976.

(49) Jin, D.; Wek, S. A.; Cordova, R. A.; Wek, R. C.; Lacombe, D.; Michaud, V.; Musier-Forsyth, K. Aminoacylation-defective bi-allelic mutations in human EPRS1 associated with psychomotor developmental delay, epilepsy, and deafness. *Clinical Genetics* **2023**, *103* (3), 358-363.

(50) Kurata, K.; James-Bott, A.; Tye, M. A.; Yamamoto, L.; Samur, M. K.; Tai, Y.-T.; Dunford, J.; Johansson, C.; Senbabaoglu, F.; Philpott, M. Prolyl-tRNA synthetase as a novel therapeutic target in multiple myeloma. *Blood Cancer Journal* **2023**, *13* (1), 12.

(51) Yoon, I.; Kim, S.; Cho, M.; You, K. A.; Son, J.; Lee, C.; Suh, J. H.; Bae, D. J.; Kim, J. M.; Oh, S. Control of fibrosis with enhanced safety via asymmetric inhibition of prolyl-tRNA synthetase 1. *EMBO Molecular Medicine* **2023**, e16940.

(52) Jandourek, O.; Tauchman, M.; Paterova, P.; Konecna, K.; Navratilova, L.; Kubicek, V.; Holas, O.; Zitko, J.; Dolezal, M. Synthesis of Novel Pyrazinamide Derivatives Based on 3-Chloropyrazine-2-carboxamide and Their Antimicrobial Evaluation. *Molecules* **2017**, *22* (2), 223.

(53) Franzblau, S. G.; Witzig, R. S.; McLaughlin, J. C.; Torres, P.; Madico, G.; Hernandez, A.; Degnan, M. T.; Cook, M. B.; Quenzer, V. K.; Ferguson, R. M. Rapid, low-technology MIC determination with clinical Mycobacterium tuberculosis isolates by using the microplate Alamar Blue assay. *Journal of clinical microbiology* **1998**, *36* (2), 362-366.

(54) Jumper, J.; Evans, R.; Pritzel, A.; Green, T.; Figurnov, M.; Ronneberger, O.; Tunyasuvunakool, K.; Bates, R.; Žídek, A.; Potapenko, A. Highly accurate protein structure prediction with AlphaFold. *Nature* **2021**, *596* (7873), 583-589.

(55) Stumpe, M. C.; Blinov, N.; Wishart, D.; Kovalenko, A.; Pande, V. S. Calculation of local water densities in biological systems: a comparison of molecular dynamics simulations and the 3D-RISM-KH molecular theory of solvation. *The journal of physical chemistry B* **2011**, *115* (2), 319-328.

6. REPRESENTATIVE NMR SPECTRA

Compound – 1 (4-Me-LAC)

^{1}H NMR (600 MHz, CHLOROFORM-D) δ 8.97 (d, J = 2.1 Hz, 1H, PzH), 8.82 (d, J = 2.1 Hz, 1H, PzH), 8.49 – 8.17 (m, 2H, ArH), 7.45 – 7.31 (m, 2H, ArH), 2.47 (s, 3H, MeH).

^{13}C NMR (151 MHz, CHLOROFORM-D) δ 161.64, 157.49, 155.15, 151.57, 145.65, 145.49, 130.47, 129.99, 129.60, 126.14, 22.00.

Compound – 8 (4t-butyl E)

¹H NMR (600 MHz, DMSO-*D*₆) δ 11.31 (s, 1H, NHCO), 8.71 (d, *J* = 2.4 Hz, 1H, PzH), 8.55 (d, *J* = 2.4 Hz, 1H, PzH), 8.01 – 7.91 (m, 2H, ArH), 7.63 – 7.48 (m, 2H, ArH), 3.75 (s, 3H, OMeH), 1.32 (s, 9H, tBuH).

¹³C NMR (151 MHz, DMSO-*D*₆) δ 165.94, 164.92, 155.56, 145.99, 145.16, 139.70, 138.39, 130.14, 127.99, 125.38, 52.33, 34.78, 30.85.

Compound – 14 (2Me, 4F NH₂)

¹H NMR (600 MHz, DMSO-*D₆*) δ 12.18 (s, 1H, NHCO), 8.62 (d, *J* = 2.5 Hz, 1H, PzH), 8.52 (s, 1H, CONH), 8.42 (d, *J* = 2.5 Hz, 1H, PzH), 8.07 (s, 1H, CONH), 7.68 (dd, *J* = 8.6, 5.9 Hz, 1H, ArH), 7.23 – 7.14 (m, 2H, ArH), 2.46 (s, 3H, CH3).

| A (s) 12.18 | | C (s) 8.52 | F (dd) 7.68 | | | H (s) 2.46 |
| B (d) 8.62 | E (s) 8.07 | G (m) 7.19 |
| D (d) 8.42 |

¹³C NMR (151 MHz, DMSO-*D₆*) δ 167.79, 165.44, 162.86 (d, *J* = 247.8 Hz), 148.17, 145.74, 140.17 (d, *J* = 8.6 Hz), 137.92, 132.38 (d, *J* = 3.1 Hz), 132.10, 129.77 (d, *J* = 9.3 Hz), 117.82 (d, *J* = 21.5 Hz), 112.82 (d, *J* = 21.5 Hz), 19.63.

B (s) 165.44	E (s) 145.74	K (s) 132.10	I (d) 112.82	M (s) 19.63
A (s) 167.79	D (s) 148.17	G (s) 137.92	H (d) 117.82
C (d) 162.86	F (d) 140.17	J (d) 129.77
		L (d) 132.38

THE END